International Journal of Engineering and Geosciences (IJEG),
Vol;2, Issue;01, pp. 1-8, February, 2017, ISSN 2548-0960, Turkey,
DOI: 10.26833/ijeg.285770

LEAST COST PATH ALGORITHM DESIGN FOR HIGHWAY ROUTE SELECTION

Sarı, F.,[1]* Şen, M.,[2]

[1] Selcuk University, Çumra School of Applied Science, Management Information Systems Department (fatihsari@selcuk.edu.tr)

[2] The General Directorate of Cadastre and Land Registry, Konya, Turkey (mehmetsenxyzku@yahoo.com)

*Corresponding Author, Received: 12/01/2017, Accepted: 30/01/2017

ABSTRACT: Highway route design is a difficult process due to the complex structure of the environment. The topography and the natural geographical objects constitute an obstacle for highway constructions. On the other hand, the cost parameter and protecting the environment are main two issues which planners have to consider. Thus, the priorities of the highway routes should be decided according to the requirements and expectations. At this point, Least Cost Path Algorithm (LCPA) makes it possible to investigate least cost path for highway routes. This cost can be assigned as the cost of the constructions such as avoiding slope and swampy areas or an environmental object such as keeping the forests and not damaging to agricultural lands. When the cost parameter is decided, then LCPA can calculate the least cost path from origin point to destination. In this study, new highway routes are investigated for Konya city with economic, environmentally and hybrid approaches. The cost parameter and related surfaces are generated according to the highway construction requirements and then with LCPA, three different routes are calculated. The result maps are generated and the three approaches are compared for
environmental and cost parameters.

Keywords: *Least Cost Path Algorithm, Geographical Information Systems, Site Selection, Highway Projects*

1. INTRODUCTION

The highway planning has some conflicts between economic and environmental perspective. Considering the cost parameter can have negative effects to the environment and habitat due to the demonstrated forests, changed water resources directions, construction wastes, air pollution and noise. On the other hand, environmental oriented highway projects can increase the cost due to the higher slope and height values together with the increased length.

Due to the negative effects of highway projects to the environment, considerably, the cost of the projects is getting increased. The environmental and cost priorities of the highway projects must be considered when examining the most suitable highway routes. The environmental or cost oriented highway projects can be defined with Analytical Hierarchy Process (AHP).

AHP is the most mentioned methods in multi-criteria analysis and is a general term that refers to the applications used to determine the most suitable solution to the real problems by providing a selection from different data clusters (Arentze and Timmermans, 2000). For determining the most suitable highway locations, AHP includes flexible, effective and adjustable structure to provide user-defined solutions. Thus, the results can be adjusted, evaluated and measured both environmental and cost oriented approaches (Kara and Usul, 2012).

Beside AHP, least-cost path analysis (LCPA) algorithm is used to determine the route alternatives of highways. LCPA provides users to find a cheapest route that connects two locations with using a cost surface that is determined by considering multiple criteria (Hassan and Effat, 2013). The cost surface can be produced via Geographical Information Systems (GIS) and the cost criteria can be evaluated and weighted with AHP. Some of the studies on LCPA involve a selecting the fastest path with the least slope (Stefanakis and Kavouras, 1995), selecting three alternatives between destination and origin points (Hassan and Effat, 2013), determining arctic all weather road (Atkinson et al. 2005), optimal route from multiple destination and origin points (Lee and Stucky, 1998), multi-criteria based cost surfaces (Collischonn and Pliar, 2000) and (Douglas, 1994).

The studies show that suitable highway locations and routes should be determined with AHP and LCPA integration for real solutions. While AHP determines the most suitable locations, LCPA decides the route considering the weights of parameters that calculated with AHP. AHP provides cost surface to the LCPA such as environment, economic and social, thus, the routes can be determined with LCPA according to the desired parameter oriented approach.

In this study, the most suitable highway locations are determined with AHP and 3 routes are determined where new highway needed according to the environment, economic and AHP which is a combination environment and cost parameters.

2. MATERIALS AND METHOD

2.1. Study Area

The Konya city is located in the middle of Turkey and in the 40814 km2 area, it is the largest city of Turkey with its 31 districts (Figure 1). The population of Konya is 2.108.808 according to the 2014 Census (URL 1). A large amount of the population is settled in the city center and has a rapidly increasing population trend with % 6.

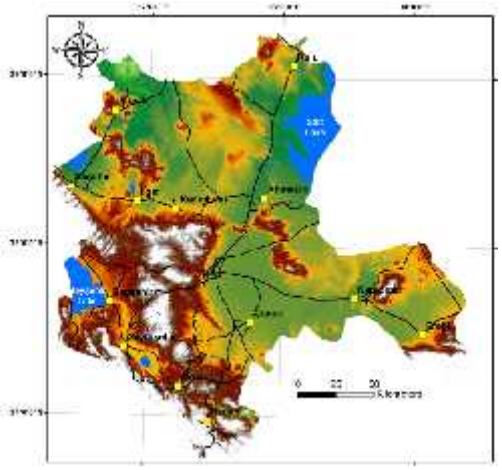

Figure 1 Study area

2.2. Least Cost Path Algorithms

In practice, the majority of routing methods are based on least-cost algorithms. The link cost is defined on both directions between each pair of nodes. Several least-cost-path algorithms have been developed for packet-switched networks. In particular, Dijkstra's algorithm and the Bellman-Ford algorithm are the most effective and widely used algorithms (Nader, 2006).

2.3. The Dijkstra algorithm

Dijkstra's algorithm is a centralized routing algorithm that maintains information in a central location. The objective is to find the least-cost path from a specified source node to all other nodes. This algorithm determines least-cost paths from a origin node to a destination node by optimizing the cost in multiple iterations. Dijkstra's algorithm is as follows : (Rees, 2004),

1. Assign a definite cost of zero to the target cell.

2. Identify all the neighbouring cells to the target cell and place them in the list of 'active' cells. For each of these cells, calculate and assign the cost of reaching the target cell, and assign a pointer that points to the target cell;

3. Find the cell in the list that has the lowest cost, Name this cell as ***C*** and the cost as ***k;***

4. Determine all the neighbouring cells of ***C*** as ***S.*** For each cell ***C'*** in ***S***, calculate the cost ***l*** of moving to ***C***.

   4.1. If ***C*** is not included of the list, add it to the list with a cost ***k + l*** and a pointer that points to ***C.***

   4.2. If ***C*** is already a member of the list, compare the value of ***k + l*** with the provisional cost of this cell. If ***k + l*** is greater than or equal to the provisional cost, do nothing. However, if ***k + l*** is less than the provisional cost, change the attributes of the cell C so that its cost is now ***k +l*** and its pointer now points to the cell C.

5. Change the attributes of the cell C from provisional to definite, and remove it from the list.

6. Repeat from (3) until the list is empty (Rees, 2004), (Dijkstra, 1959).

2.4. How cost distance works (ArcGIS Example)

The cost to travel between one node and the next is dependent on the spatial orientation of the nodes. How the cells are connected also impacts the travel cost (URL 2). The topology is being important in this cost calculation. When moving from a cell to one of its four directly connected neighbours, the cost can be calculated as;

a1 = (cost1 + cost2) / 2

where:
cost1, The cost of cell 1
cost2, The cost of cell 2
a1, The total cost of the link from cell 1 to cell 2

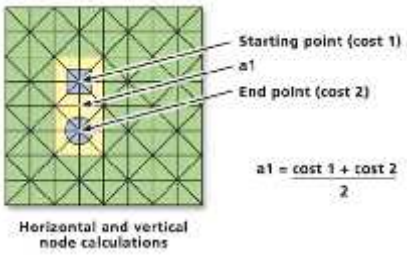

Figure 2 Adjacent nodes

The accumulative cost can be determined by the following formula:

accum_cost = a1 + (cost2 + cost3) / 2

where:
cost2; The cost of cell 2
cost3; The cost of cell 3
a2; The cost of moving from cell 2 to 3
accum_cost; The accumulative cost to move into cell 3 from cell 1

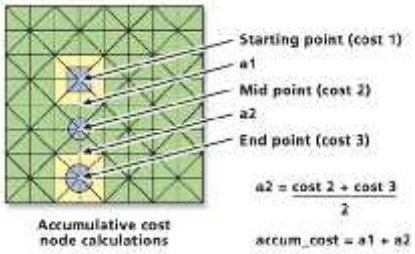

Figure 3 Perpendicular nodes

If the movement is diagonal, the cost to travel over the link can be calculated with; (1.41421 is square root of 2);

a1 = 1.414214 (cost3 + cost2) / 2

When determining the accumulative cost for diagonal movement, the following formula must be used

accum_cost = a1 + 1.414214(cost2 + cost3) / 2

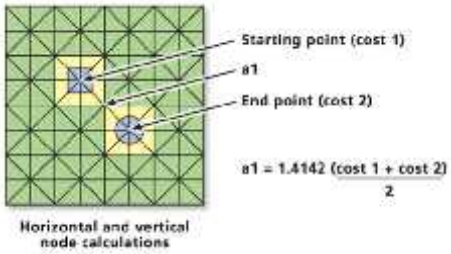

Figure 4 Diagonal nodes

Creating a cost-distance raster using graph theory can be viewed as an attempt to identify the lowest-cost cell. It is an iterative process that begins with the source cells. The goal of each cell is to be assigned quickly to the output cost-distance raster (URL 2).

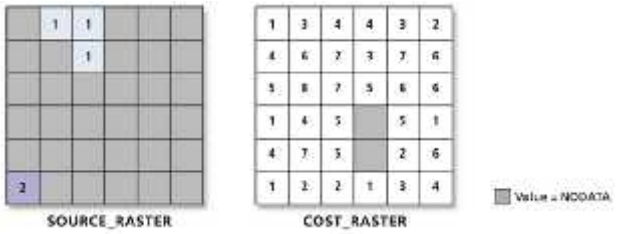

Figure 5 Accumulative cost cells

In the first iteration, the source cells are identified and assigned 0 since there is no accumulative cost to return to themselves. Next, all the source cell's neighbours are activated, and a cost is assigned to the links between the source cell nodes and the neighbouring cells' nodes using the above accumulative cost formulas. To be

assigned to the output raster, a cell must have the next least-cost path to a source (URL 2).

The accumulative cost values are arranged in a list from the lowest accumulative cost to the highest (Figure 6).

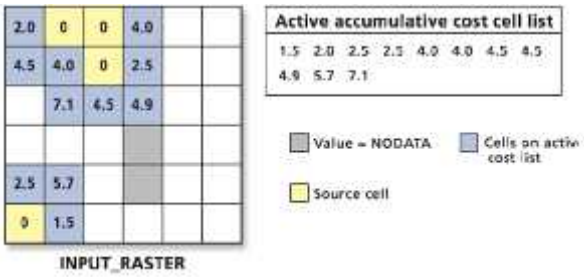

Figure 6 Cost calculation first stage

The lowest cost cell is chosen from the active accumulative cost cell list, and the value for that cell location is assigned to the output cost-distance raster. The list of active cells expands to include the neighbours of the chosen cell, because those cells now have a way to reach a source. Only those cells that can possibly reach a source can be active in the list. The cost to move into these cells is calculated using the accumulative cost formulas (URL 2).

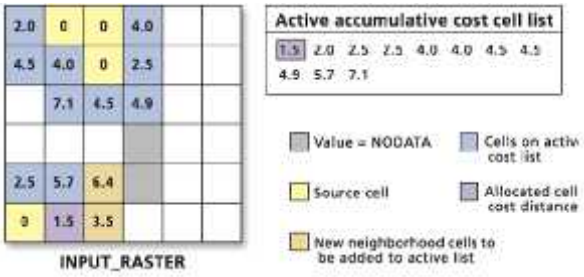

Figure 7 Cost calculation second stage

Again, the active cell on the list with the lowest cost is chosen, the neighbourhood is expanded, the new costs are calculated, and the new cost cells are added to the active list. Source cells do not have to be connected. All disconnected sources contribute equally to the active list. Only the cell with the lowest accumulative cost is chosen and expanded, regardless of the source to which it will be allocated (URL 2).

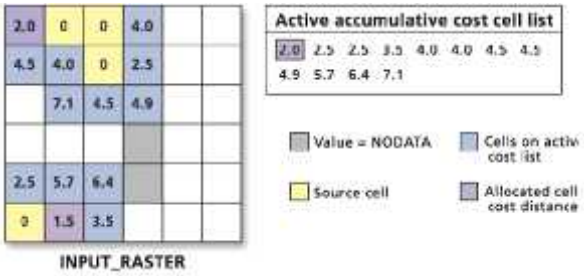

Figure 8 Cost calculation third stage

This allocation process continues. Furthermore, cells on the active list are updated if a new, cheaper route is created by the addition of new cell locations to the output raster (URL 2).

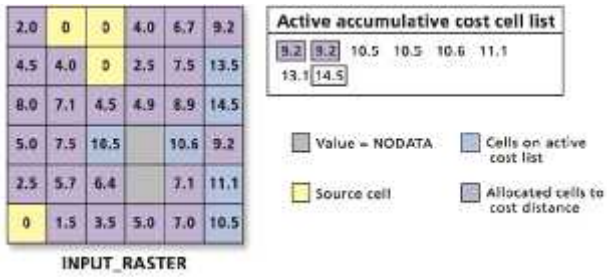

Figure 9 Cost calculation final stage

While the output cost distance raster identifies the accumulative cost for each cell to return to the closest source location, it does not show which source cell to return to or how to get there. The Cost Back Link process returns a direction raster as output, providing what is essentially a road map that identifies the route to take from any cell, along the least-cost path, back to the nearest source (URL 3).

The algorithm for computing the back link raster assigns a code to each cell. The code is a sequence of integers from 0 to 8. The value 0 is used to represent the source locations, since they have essentially already reached the goal (the source). The values 1 through 8 encode the direction in a clockwise manner starting from the right. Following is the default symbology applied to the directional output, accompanied by an arrow diagram matching directional arrows to the color symbology (URL 3):

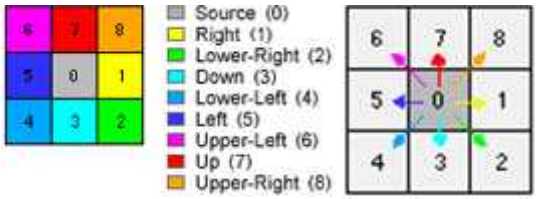

Figure 10 Back link raster calculation

2.5. AHP Application

The criteria selection reflects the requirements, expectations and restrictions of highway constructions. The main criteria of highway projects can be divided into two categories as like environment and economic. Each criterion will be weighted with AHP to decide the most suitability highway routes according to the defined scores. Evaluating for economic criteria, highway routes are expected to be in quite flat lands from avoiding excavation costs. Height criterion is related to slope criterion and considering the climate conditions, it

defines the characterization of highway route. If a highway has a high height, it will be negatively affected from climate conditions like perception, snow, wind and ice in winter. Height is also increasing the excavation costs and the slope of the highway route. This mean increased fuel consumption, particularly for transportation vehicles.

The environmental criteria are critical for highway routes to protect the environment and habitat. Highway constructions can destroy the forest and fertile agricultural lands. Addition to this, the habitats and migration routes of animals can be damaged due to the vehicle flow, sound, exhaust emissions and related air pollutants. First of all, the purpose of the project aim must be demonstrated that the priority will be protecting the environment or the cost. AHP can define this distinction easily with the pair-wise comparison matrix. (Saaty, 1977). The procedure outlined by Saaty (1977, 1980) scales the importance of each criterion, from 1 to 9 relatively.

The pair-wise comparison square matrix is defined for main-criteria, criteria and sub -criteria to determine the weights. The diagonal elements of the comparison matrix are 1. Each element of the comparison matrix is divided to the sum of the own column sum to generate a normalized matrix with Formula 1.

$$a_{ij}^{1} = \frac{a_{ij}}{\sum_{i=1}^{n} a_{ij}} \quad (1)$$

Each column of the normalized matrix sum is equal to 1. Then, each row sum of the normalized matrix is divided to the matrix order. The average of the sum represents the weights of each criterion in pair-wise comparison matrix (Formula 2).

$$w_i = \left(\frac{1}{n}\right) \sum_{j=1}^{n} a_{ij} \; (i,j = 1,2,3,\ldots,n) \quad (2)$$

The consistency of the pair-wise comparison matrix must be calculated to decide the criteria comparisons are consistent or not. The assigned preference values are synthesized to determine a ranking of the relevant factors in terms of a numerical value which is equivalent to the weights of each parameter. Therefore, the eigenvalues and eigenvectors of the square pair-wise comparison matrix revealing important details about patterns in the data matrix are calculated. It is regarded sufficient to calculate only the eigenvector resulting from the largest eigenvalue since this eigenvector contains enough information to the relative priorities of the parameters being considered (Saaty& Vargas 1991).

Consistency Index (CI) is one of the methods to define the consistency coefficient of pair-wise comparison matrix. CI is calculated with Formula 3 (Saaty, 1994).

$$CI = \frac{\lambda_{max} - n}{n-1} \quad (3)$$

Calculating consistency index depends the λmax (eigen value) value with Formula 4 (Saaty, 1994).

$$\lambda_{max} = \frac{1}{n} \sum_{i=1}^{n} \left[\frac{\sum_{j=1}^{n} a_{ij} w_j}{w_i} \right] \quad (4)$$

Addition to this, random index (RI) value must be calculated to determine consistency index. For each matrix order, RI values are given in Table 1.

Table 1. RI values according to the matrix order

n	1	2	3	4	5	6	7	8	9	10
RI	0	0	0,58	0,90	1,12	1,24	1,32	1,41	1,45	1,49

After calculating the CI and RI, consistency ratio (CR) can be calculated with Formula 5. If CR exceeds 0.1, based on expert knowledge and experience, Saaty& Vargas (1991) recommend a revision of the pair-wise comparison matrix with different values. (Saaty, 1980).

$$CR = \frac{CI}{RI} \quad (5)$$

Several criteria should be considered when selecting highway routes. In this study, 7 criteria are considered within 2 main criteria, environmental and economic. Slope, distance from highways, height and population criteria are included in economic main criteria which are affecting the cost of the highway projects. Distance from settlements, land use and geology criteria are related to the respect to the environment (Figure 11).

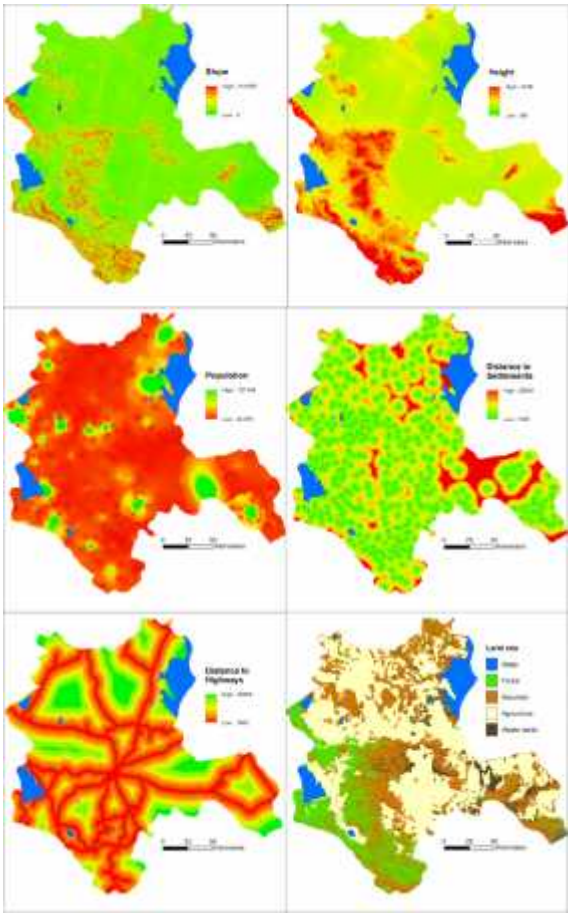

Figure 11 Criteria maps

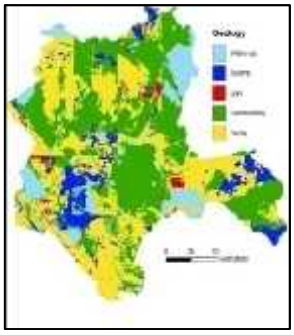

Figure 11 Criteria maps

Each criterion is mapped and then reclassified with ArcGIS software according to the defined classes which are illustrated in Figure 11. These are defined as sub-criteria and AHP weights. are calculated for the main-criteria, criteria and sub-criteria In first stage, environmental and economic main criteria are weighted with pair-wise comparison matrix which is given in Table 3,4.

Table 2. Main criteria weights

A	C_1	C_2	*W*
C_1	1	0.6666	0.40
C_2	1/0.6666	1	0.60

A=Highway suitability C1= Environmental,
C2= Economic, CR=0.0000, W=Weights of C1 and C2

The main-criteria weights are calculated as 0,40 for C1 and 0,60 for C2 (Table 2). Therefore, economic criteria are more important than environmental criteria for this study.

In second stage, criteria weights are calculated separately according to the main-criteria. The CR values of all comparisons are lower than 0.10, which indicated that the use of the weights are suitable (Table 3,4).

Table 3.Economic criteria weights

B_1	C_3	C_4	C_5	*W*
C_3	1	2	2	0.49981
C_4	1/2	1	1.1	0.25804
C_5	1/2	1/1.1	1	0.24215

B1= Economic criteria, C3= Slope,
C4=Height, C5= Geology, CR=0,0009
W=Weights of C3, C4 and C5

Table 4.Environmental criteria weights

B_2	C_6	C_7	C_8	C_9	*W*
C_6	1	2.5	2.2	1.6	0.40156
C_7	1/2.5	1	1.2	2.2	0.24719
C_8	1/2.2	1/1.2	1	1.4	0.18646
C_9	1/1.6	1/2.2	1/1.4	1	0.16479

B2= Environmental criteria, C6= Land, C7=Population,
C8= Distance to settlements C9=distance to highways, CR=0,0498 W=Weights of C6, C7,C8 and C9

2.6. Least-Cost Path Algorithm Application

Least Cost path Algorithm is generated by ArcGIS software with using spatial analyst extension. Totally, 3 routes are calculated with LCPA which are determined the most highway required locations with AHP (Figure 12). There are 3 cost surfaces is determined for LCPA to calculate the least cost path between origin and destination points. The origin and destination points are specified with calculating the intersection of existing highways in districts.

The least cost paths are determined for economic, environmental and AHP calculations separately. The weights that are determined with AHP (Table 2,3,4) are used to generate the cost surfaces. The cost surfaces are calculated as follows,

Economic cost surface = [(0.49981 X Slope) + (0.25804 x Height) + (0.24215 x Geology)]

Environmental cost surface = [(0.40156 x Land use) + (0.24719 x Population) + (0.18646 x Dist_from_settlements) + (0.16479 x Dist_from_highways)]

AHP cost surface = [(0.30 X Slope) + (0.1548 x Height) + (0.145 x Geology) + (0.1606 x Land use) + (0.0988 x Population) + (0.074 x Dist_from_settlements) + (0.0658 x Dist_from_highways)]

Deciding the most suitable path requires a comparison of the routes according to the length, slope, land use and population. The AHP routes can be called as hybrid route because it combines both economic and environmental criteria together. AHP route is calculated with % 60 economic and %40 environmental criteria. According to the aim, these weights can be changed considering the requirements as like cost or environment oriented highway constructions. The AHP, Economic and Environment oriented cost surfaces are given in Figure 12.

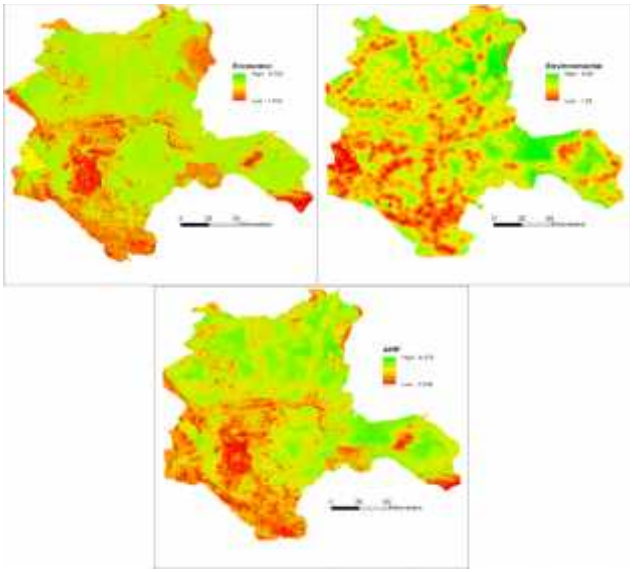

Figure 12 Cost surfaces for economic, environment and AHP

The origin and destination points are defined considering the existing highways and intersection of highways which connect the districts. The back link raster must be generated to be able to calculate the least cost paths. The back link rasters include the directions of raster cells to each other by considering the origin and destination points. The rasters are given in Figure 13.

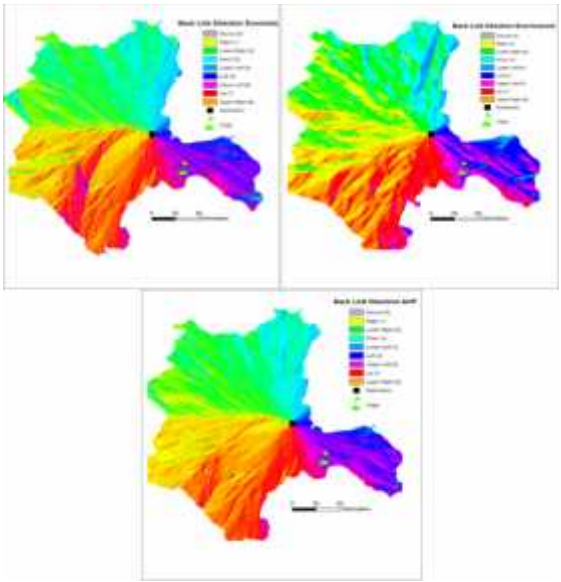

Figure 13 Back link rasters for economic, environment and AHP

The determined suitable locations are used to generate LCPA paths for economic, environmental and AHP oriented approach (Figure 14). There are 3 LCPA routes are determined for mentioned location. The routes tend to be close each other considering the homogeneous geographical distributions of the criteria.

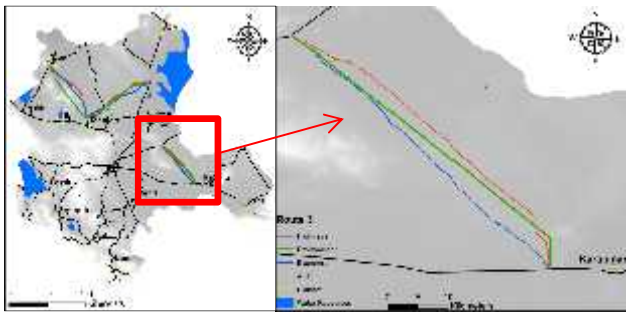

Figure 14 LCPA routes

Profiles of the routes are generated via ArcGIS software to compare the heights of routes. The profiles are given in Figure 15 for Route 1, Route 2 and Route 3). The vertical axis of the graph represents the altitude (meter) and the horizontal axis represents the length (kilometer) of the determined route.

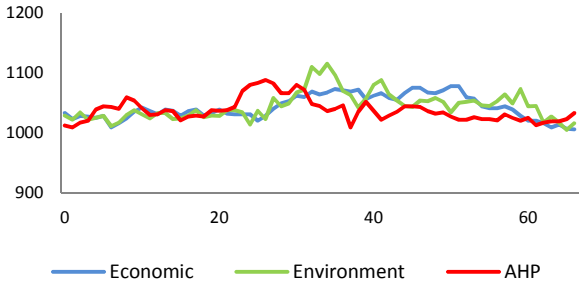

Figure 15 Height profiles of the LCPA routes

3. RESULTS

The results show that determined most suitable highway locations are quite enough to decide highway routes together with LCPA integration. Instead of deciding cost oriented routes, the hybrid AHP routes are more appropriate for projects. However, the suitable highway locations should be investigated with environment oriented routes and then compared with economic oriented routes.

The routes should be investigated and minor modifying can be processed on highway routes. Especially in economic routes, the LCPA determined the routes within less slope and height. Thus, the routes can be intersected with the water collect and flow lines of the mountains and hills. This will increase the cost due to the new construction requirement such as culverts and drainage structures. The crossroads and intersection points according to the settlements can be easily decided by an investigation process on determined highway routes.

REFERENCES

Arentze, T. A. and Timmermans, H. J. P., 2000. ALBATROSS: A Learning-based Transportation Oriented Simulation System. EIRASS, Eindhoven University of Technology, The Netherlands.

Atkinson, D.M., Deadman, P., Dudycha, D., Traynor, S., 2005. Multi-criteria evaluation and least cost path analysis for an arctic all-weather road. Appl. Geogr. 25, 287–307.

Collischonn, W., Pilar, J.V., 2000. A directional dependent least-cost path algorithm for roads and canals. Int. J. Geogr. Inform. Sci. 14 (4), 397–406.

Dijkstra, E.W., 1959. A note on two problems in connection
with graphs. Numerische Mathematik 1, 269–271.

Douglas, D.H., 1994. Least cost path in GIS using an accumulated cost surface and slope lines. Cartographica 31 (3), 37–51.

Hassan, O., Effat, H., (2013). Designing and evaluation of three alternatives highway routes using the Analytical Hierarchy Process and the least –cost path analysis, application in Sinai Peninsula, Egypt. The Egyptian Journal of Remote Sensing and Space Sciences, 16, 141-151.

Kara, F., Usul, N., 2012. Highway Route Design Through The Use Of GIS AndMulticriteria Analysıs: A Case Study Of Istanbul. Ozean Journal of Applied Sciences 5(1), 71-84.

Lee, J., Stucky, D., 1998. On applying viewshed analysis for determining least-cost paths on digital elevation models. Int. J. Geogr. Inform. Systems 12 (8), 891–905.

Nader, M, F., 2006. Computers and Communication Networks, Prentice Hall, ISBN-13: 978-0131389106.

Rees, W.G., 2004. Least cost paths in mountainous terrain. Computers & Geosciences, 30, 203-209.

Saaty, T. L., 1977. A scaling method for priorities in hierarchical structures. Journal of Mathematical Psychology, 15, 234–281.

Saaty, T. L. 1980. The analytical hierarchy process. New York: Wiley.

Saaty, T. L. 1994. Fundamentals of Decision Making and Priority Theory With The Analytical Hierarchy Process, RWS Publ. Pittsburg, ,s 69-84, 1994.

Saaty, T.L., Vargas, L.G., 1991. Prediction, Projection and Forecasting. Kluwer Academic Publishers, Dordrecht, 251 pp.

Stefanakis, E., Kavouras, M., 1995.On the determination of the optimum path in space. In: Proceedings of the European Conference on Spatial Information Theory, COSIT 95, Lecture Notes in Computer Science. Springer, Berlin.

URL 1, Turkish Statistical Institute Official website, http://www.tuik.gov.tr/Start.do , (Last visited 11.01.2016).

URL 2 Arcgis Help Center, http://desktop.arcgis.com/en/arcmap/10.3/tools/spatial-analyst-toolbox/how-the-cost-distance-tools-work.htm#ESRI_SECTION1_F6B0C27F739748A5BD6C8E4BB651E453

URL 3 Arcgis Help Center, http://desktop.arcgis.com/en/arcmap/10.3/tools/spatial-analyst-toolbox/understanding-cost-distance-analysis.htm

International Journal of Engineering and Geosciences (IJEG),
Vol;2, Issue;01, pp. 9-16, February, 2017, ISSN 2548-0960, Turkey,
DOI: 10.26833/ijeg.286003

COMPARING UNIFORM AND RANDOM DATA REDUCTION METHODS FOR DTM ACCURACY

Yilmaz, M., [1]* Uysal, M., [1]

[1] Afyon Kocatepe University, Engineering Faculty, Department of Geomatic Engineering, TR-03200 Afyonkarahisar, Turkey (mustafayilmaz, muysal@aku.edu.tr)

*Corresponding Author, Received: 16/01/2017, Accepted: 28/01/2017

ABSTRACT: The digital cartographic representation of the elevation of the earth's surface created from discrete elevation points is defined as a digital terrain model (DTM). DTMs have been used in a wide range of applications, such as civil planning, flood control, transportation design, navigation, natural hazard risk assessment, hydraulic simulation, visibility analysis of the terrain, topographic change quantification, and forest characterization. Remote sensing, laser scanning, and radar interferometry become efficient sources for constructing high-accuracy DTMs by the developments in data processing technologies. The accuracy, the density, and the spatial distribution of elevation points, the terrain surface characteristics, and the interpolation methods have an influence on the accuracy of DTMs. In this study, uniform and random data reduction methods are compared for DTMs generated from airborne Light Detection and Ranging (LiDAR) data. The airborne LiDAR data set is reduced to subsets by using uniform and random methods, representing the 75%, 50%, and 25% of the original data set. Over the Mount St. Helens in southwest Washington State as the test area, DTM constructed from the original airborne LiDAR data set is compared with DTMs interpolated from reduced data sets by Kriging interpolation method. The results show that uniform data reduction method can be used to reduce the LiDAR datasets to 50% density level while still maintaining the quality of DTM.

Keywords: *DTM, LiDAR, Uniform, Random, Kriging.*

1. INTRODUCTION

A digital elevation model (DEM) is defined as the digital cartographic representation of the elevation of the earth's surface in all its forms. The generic DEM normally implies elevations of the terrain void of vegetation and man-made features. This bare-earth DEM is is generally synonymous with a digital terrain model (DTM). DTMs frequently incorporate the elevation of the significant topographic features of the land, plus mass points and breaklines that are irregularly spaced so as to better characterize the true shape of the bare earth terrain (Maune et al., 2007). DTMs provide a three-dimensional (3D) representation of the bare earth/underlying terrain of the earth's surface that contains elevations of topography (ridgelines, stream courses, breaklines, etc.) where vegetation, buildings, and other non-ground objects have been removed. DTMs have found wide application in all geosciences and engineering tasks such as: civil planning, mine engineering, military purposes, landscape design, urban planning, environmental protection, forest characterization, hydraulic simulation, visibility analysis of the terrain, surface modelling, topographic change quantification, volume computation, geomorphological extraction, satellite imagery interpretation, cartographic presentation, and geographical analysis (Li et al., 2005; Tarolli et al., 2009; Cavalli and Tarolli, 2011). DTMs can be derived by field surveying, photogrammetry or cartographic digitization of existing topographic maps. Besides the conventional methods for creating DTMs, new technologies such as satellite remote sensing, radar interferometry and airborne laser scanning revolutionize the construction of high quality DTMs in a cost-effective manner. Due to advancements in reliability and spatial resolution over the past decades, airborne Light Detection and Ranging (LiDAR) is becoming the privileged data acquisition technique for high-resolution and high-accuracy DTMs over large areas owing to providing 3D non-uniformly spaced dense point information very effectively (Ma and Meyer, 2005; Liu, 2008; Vianello et al., 2009; Razak et al., 2011; Arab-Sedze et al., 2014, Polat and Uysal, 2015; Yan et al., 2015). LiDAR has become a well-established resource used to enhance spatial knowledge of the topography in order to construct DTMs while preserving high frequencies of the relief. The spatial distribution of usable data points is expected to be uniform for DTM construction in a broad application spectrum. Although, LiDAR do not produce regularly gridded points. The output of a LiDAR survey is a point cloud of hundreds of millions or billions of sample points representing the feature height. Each laser point is randomly located. In many cases, not all points may be required for defining the terrain surface. Therefore, the raw point clouds need to be processed (filtering and interpolation) in order to provide an approximation to a real-world continuous surface (Garnero and Godone, 2013).

The accuracy of the features derived from DTMs depends on several factors originating from: (i) the accuracy, the density, and the spatial distribution of elevation points, (ii) the interpolation methods, (iii) the terrain surface characteristics (Gong et al., 2000; Chen and Yue, 2010; Liu et al., 2011; Sailer et al., 2014). The first two factors are clearly errors (the objective problems with measurement/estimation), whereas the third should be considered a matter of uncertainty (less tangible issues). Alternatively, the first can be regarded as data-based, being strictly concerned with the source data, while the second and the third are model-based, being concerned with how well the resulting DTM approximates the real physiography (Fisher and Tate, 2006). There has been extensive literature about these factors: the accuracy of data acquisition (Hodgson and Bresnahan, 2004; Rayburg et al., 2009; Mukherjee at al., 2013; Dorn et al., 2014); the data density (Aguilar et al., 2005; Chaplot et al., 2006; Liu et al., 2007); the spatial distribution of source data (Erdogan, 2010; Gumus and Sen, 2013; Fassnacht et al., 2014); the interpolation process (Yilmaz, 2007; Chen and Li, 2012; Arun, 2013; Tan and Xu, 2014); the terrain features (Aguilar et al., 2007; Aguilar and Mills, 2008; Chu et al., 2014).

The contemporary airborne LiDAR systems can operate between 150.000 to 400.000 laser pulses per second, where achieved density (measurement resolution) exceeds 10 points per square meter (Renslow, 2012). Nowadays, there are even 1 GHz (1.000.000 laser pulses) airborne LiDAR sensors available. The use of LiDAR has rapidly become a standard source of elevation data for building high quality DTMs. The DTM resolution has increased dramatically in the recent years as a consequence of higher LiDAR point densities. Modern LiDAR sensors allow simultaneously capturing topographic and bathymetric details from large geographical areas at the price of a highly increased data volume. When DTM of different resolution is required the common technique is removing data to produce a coarser resolution data set. Besides, the production of different horizontal resolution DTM from the same data source is important for predicting scale dependent environmental variables. The use of LiDAR offers the flexibility needed to produce multiple horizontal resolutions of DTM from the same data source. However, the high-density LiDAR data lead to a significant increase in the data volume, imposing challenges with respect to data storage, processing, and manipulation for producing DTM. Because of the copious number of LiDAR spot elevations returned on an areal basis, the effects of data density reduction on DTM of various horizontal resolutions is worthy of study, particularly for landscape scale studies. With a data reduction, a more manageable and operationally sized elevation data set is possible (Anderson et al., 2006). Therefore, terrain data reduction (achieving an adjustment between density of data and volume of data) without losing relevant geometric details has become a research topic while constructing DTMs. However, there are particularly limited studies about data reduction for DTMs (e.g., Anderson et al., 2005; Anderson et al., 2006; Liu et al., 2007; Liu and Zhang, 2008; Immelman and Scheepers, 2011). The main objectives of this study are to:

- Evaluate the effect of the data reduction algorithms on the accuracy of LiDAR-derived DTM construction.
- Examine to what extent a set of LiDAR data can be reduced while maintaining effectual accuracy for DTM construction.

The results of this study based on different data density are compared in terms of the mean error (ME), the mean

absolute error (MAE), and the root mean square error (RMSE) with specific reference to the study area

2. THEORETICAL BACKGROUND

2.1 Airborne LiDAR

The airborne LiDAR is an active remote sensing technique providing its own illumination and measures the ranges (variable distances) to the terrain surface of distant objects. The LiDAR sensor sends out light in the form of a pulsed laser and records the energy scattered back from the terrain surface and the objects on the terrain surface. The range is determined by measuring the round trip time between the light emission and the detection of the reflection (Wehr and Lohr, 1999). Each laser pulse may have multiple returns from features hit at different different ranges from the sensor, creating a cloud of geo-referenced points, including buildings and tree canopy, as well as elevations of bare-earth surface points. Airborne LiDAR is a multi sensor system, consisting of a laser scanner, a Global Navigation Satellite Systems (GNSS) receiver, and an inertial measurement unit (IMU). GNSS is needed to determine the 3D coordinates of the moving sensor according to one or more differential GNSS base stations. This establishes the origin of each of the thousands of laser pulses emitted each second. IMU directly measures the roll, pitch, and yaw angle of the aircraft in order to determine the angular orientation of the sensor in three dimensions in the flight. The LiDAR sensor measures the scan angle of the laser pulses. Combined with IMU data, this establishes the angular orientation of each of the thousands of pulses emitted each second. The LiDAR sensor also measures the time necessary for each emitted pulse to reflect off the ground (or aboveground features) and return to the sensor. Time translates into distance measured between the aircraft and the point being surveyed (Maune, 2008).

2.2. Data Reduction Algorithms

LiDAR based cloud consist of hundreds of millions or billions of sample points, sometimes, requires reduction without losing spatial accuracy while constructing DTMs. Through data reduction, manageable dataset, improved efficiency in storage requirements and processing time can be ensured to achieve an operational and efficient DTM. Many algorithms have been proposed to reduce the 3D point cloud data in recent years. A good survey on approaches for data reduction is given in Heckbert and Garland (1997). It is beyond the scope of this study to discuss even the most common data reduction algorithms in full detail, though the methods and modifications used within this study is provided.

Uniform data reduction (Lee et al., 2001) uniformly reduces the number of points in the point cloud by subdividing the model space into equally sized cubic cells and deletes all but remained one point from each cell. Random data reduction (Geomagic Support Center, 2014) randomly removes the points based on the specified percentage of the total points that need to be reduced. Each member of the point cloud has an equal chance of being selected (without subjectivity).

2.3. Interpolation Methods

The essential data of DTMs are the finite number of points, which have x/y coordinates with uniformly spaced z-values. Frequently, the spatial distribution of these points depends on the source of the data. The digital representation of the terrain surfaces via regular or irregular spaced points is possible by an interpolation method. Different interpolation methods applied over the same data may result in different surfaces and hence it is required to evaluate the comparative appropriateness of these techniques. The question of an optimal DTM interpolation method has stimulated several comparative studies, but there is still a lack of consensus about which interpolation method is most appropriate for the terrain data. In this paper, a commonly used interpolation method, Kriging (KRG) method is chosen.

Kriging (KRG) method (Krige, 1951) is a geostatistical and a flexible interpolation method which has been extensively used in diverse fields of mathematics, earth sciences, geography, and engineering and has proved to be powerful and accurate in its fields of use. KRG is also referred to as a linear least squares interpolation (Kraus and Mikhail, 1972) (more specialized to terrain modelling) and it is identical to simple Kriging. According to KRG, both the distance and the degree of variation between reference points are taken into account for optimal spatial prediction (Joseph, 2006). KRG assigns a mathematical function to a certain number of points or all the points located within a certain area of effect in order to determine the output values for each location (Cressie, 1991). KRG uses the semivariogram which describes the variability of data points depending on their distance and direction, and nearby values define the weights that determine the contribution of each data point to the prediction of new values at unsampled locations (Krivoruchko and Gotway, 2004). In case the semi variogram is known, KRG constitutes the best linear unbiased estimator (BLUE) (Yilmaz and Gullu, 2014).

3. STUDY AREA, SOURCE DATA, AND EVALUATION METHODOLOGY

Mount St. Helens (46^0.1912 N, 122^0.1944 W) is selected as the study area for the DTM constructions. Mount St. Helens is an active volcano located in Skamania County, Washington, in the Pacific Northwest region of the United States. It is 154 km south of Seattle, Washington, and 80 km northeast of Portland, Oregon (Fig. 1). The study area defines approximately area of 116.6 km^2. Its span is ~ 11.9 km in the north-south direction and ~ 9.8 km in the east-west direction.

Figure 1. The location of Mount St. Helens

The evaluating procedure of the DTMs refers to an original LiDAR dataset that consisting of 23071760 points (~ 5.1 m^2/point). The elevation ranges between 743.91 m and 2539.38 m, with a mean value of 1469.23 m. The data set is contained within the USGS quad Mount St. Helens, WA. The areas of interest flown at different altitudes and scanner settings depending on the area of collection. LiDAR data acquisition specifications are listed below in Table 1. Raw elevation measurements have been determined to be vertically accurate to within 15 cm. LiDAR elevation points are estimated to be horizontally accurate to 0.30 cm. The data set was evaluated against GNSS collected control points which resulted in a vertical RMSE of 0.053 m. LiDAR data were filtered by algorithms within the EarthData's proprietary software and commercial software written by TerraSolid (Mount St. Helens LiDAR Data, 2006).

	Lower Elevation	Higher Elevation
Flying altitude (m)	2133	2438
Flight speed (knots)	140	140
Laser pulse rate (kHz)	29	29
Scan angle (degrees)	± 35	± 35
Scan rate (Hz)	29	18
Swath width (m)	1345	1537

Table 1. LiDAR data acquisition specifications

In order to evaluate the effect of the data reduction algorithms on DTM accuracy and to explore the data reduction extent for adequate DTM accuracy; initially, the data density is sequentially reduced through a selection of a predetermined percentage of the original LIDAR data set. Data reduction is performed using the Geomagic Studio ® 12 software. The original LiDAR data set (100%) is reduced to a series of subsets by using uniform, curvature, grid, and random algorithms, representing the 75%, 50%, and 25% of the original LiDAR data set. This reduction protocol is similar to the previous studies of Anderson et al. (2005, 2006). Subsequent to the data reduction, the original LiDAR data set and the reduced data sets are used to produce a series of DTMs. At each data density level, DTMS are constructed via KRG interpolation method.

The evaluation of DTM accuracy is focused on the correspondent elevation differences between the reference DTM (based on the original dataset) and the test DTMs (based on the reduced datasets) using the equation below:

$$\Delta Z = Z_{(100\%)} - Z_{(i\%)} \quad (1)$$

where ΔZ is the elevation residual, Z is the elevation value of nodes estimated from (reference and test) DTMs, and i represents the data density (i = 75, 50 and 25).

For the statistical analysis of elevation differences, minimum and maximum values of ΔZ are determined and the overall performance of DTMs is assessed through ME, MAE, and RMSE accuracy measures defined by:

$$ME = \frac{1}{n}\sum_{k=1}^{n} \Delta Z \quad (2)$$

$$MAE = \frac{1}{n}\sum_{k=1}^{n} |\Delta Z| \quad (3)$$

$$RMSE = \sqrt{\frac{1}{n}\sum_{k=1}^{n} (\Delta Z)^2} \quad (4)$$

where n is the number of the points used for the accuracy verification and k refers to the residual sequence. ME is a measure of underestimation or overestimation the true value of the interpolation method. MAE provides the average deviation that DTM surface deviates from the true value to measure the effect of the data reduction on DTM accuracy. RMSE is calculated to measure the overall accuracy of DTM surface.

4. CASE STUDY

For the evaluation process, the reference DTM of the study (Fig. 2) is constructed from the original LiDAR dataset using KRG method, implemented within the Surfer ® 13 software. The accuracy of the reference DTM is assessed through cross-validation technique.

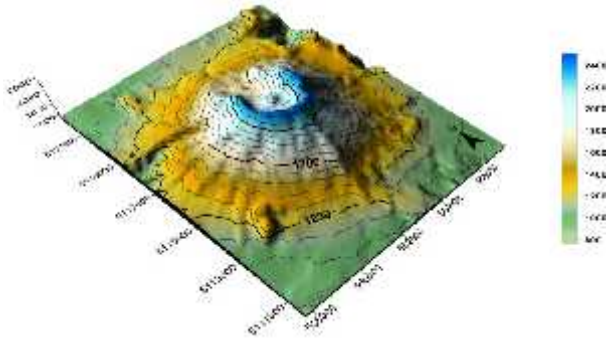

Figure 2. Reference DTM of the study area

The reduced data sets, based on uniform and random algorithms, are used to construct the test DTMs of the study area using KRG method, at each data density level (75%, 50%, and 25%). The test DTMs (DTMi%; i = 75, 50, and 25) are subtracted from the corresponding reference DTMs (DTM100%) for quantifying elevation differences. Also, the graphical representations have been adopted for the comparative evaluation of the test DTMs by producing a residual map for each test DTM

(Fig. 3) that indicates the occurrence and magnitude of elevation differences (Weng, 2006), in relation to terrain characteristics (by overlaying the contour map of Mount St. Helens on the residual maps).

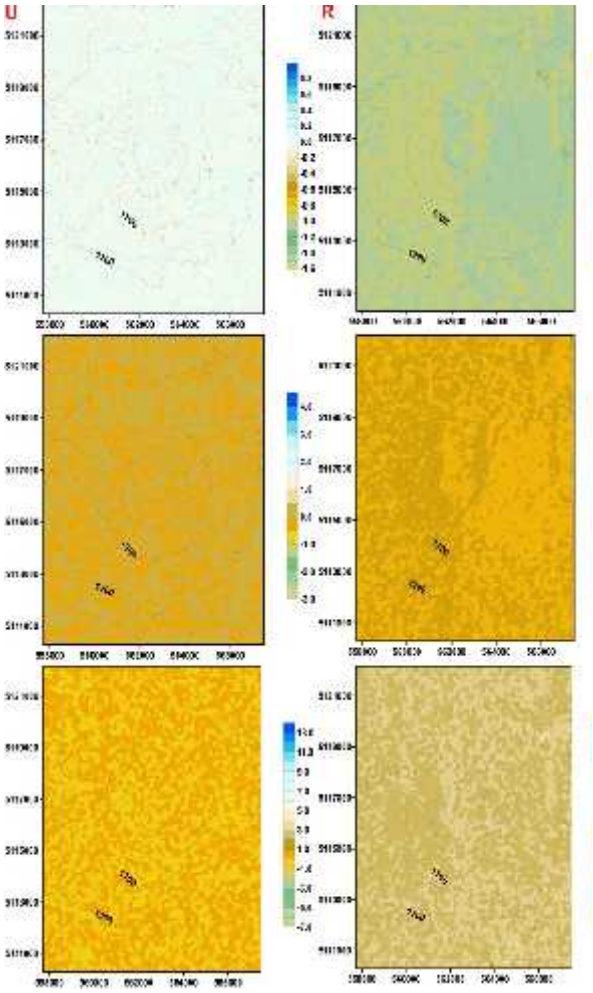

Figure 3. Residual maps of test DTMs for the study area (upper row: 100-75; middle row: 100-50; lower row: 100-75)

5. COMPARATIVE RESULTS AND CONCLUSIONS

The visual analysis of the elevation residual maps shows that the deviation of the test DTMs from the reference DTM are getting smaller depending on the increase in data density, for both data reduction algorithms. From the visual interpretation of the elevation residual maps, it is evident that uniform algorithm gave better results than random algorithm.

Global statistics of elevation residuals based on uniform and random algorithms with KRG method at selected data density levels are presented in Table 2. When the statistics summarized in Table 2 are evaluated, it can be concluded that uniform algorithm provides more accurate results than random algorithm at all data densities.

Table 2. Statistics of the elevation residuals over the study area

	UNIFORM			RANDOM		
	75%	50%	25%	75%	50%	25%
Min	-1.569	-2.837	-6.964	-3.106	-7.943	-11.587
Max	0.883	3.567	12.071	11.592	12.383	12.665
ME	-0.001	0.002	0.006	-0.005	-0.003	-0.018
MAE	0.021	0.058	0.126	0.112	0.154	0.239
RMSE	0.062	0.149	0.340	0.266	0.352	0.531

MEs are recorded at the centimetre level at 25% data density for uniform and random data reduction algorithms (0.006 m. and -0.018 m.). KRG underestimated the terrain surface because of the predominantly concentric topography of the study area. MEs are sub-centimeter at 50% and 75% data densities for uniform and random data reduction algorithms, indicating that interpolation biases were negligible.

Throughout the decreasing data densities, the test DTMs have increasing MAEs ranging from 0.021 m to 0.239 m. Terrain representations derived from the test DTMs based on uniform algorithm are better than the test DTMs based on random algorithms, at all data densities.

RMSEs ranged from 0.062 m. to 0.531 m. show significant increases for uniform and random data reduction algorithms as data densities decreased from 75% to 25%. As expected, the lowest RMSEs are obtained at 75% data density level. RMSEs of the test DTMs for data reduction algorithms have a decreasing sequence as uniform < curvature, at all data densities.

In terms of overall accuracy, there is no significant decrease for the test DTMs constructed from high data densities (75% and 50%). Hence, it becomes apparent that the test DTMs based on 75% and 50% point densities are sufficient for terrain representations

Based on the analysis results of comparison of data reduction algorithms in constructing DTMs, the following conclusions can be drawn based on this paper: (i) Uniform data reduction algorithm can be considered as a feasible technique due to better terrain representation for constructing LiDAR-derived DTMs. (ii) KRG biases are negligible with lower RMSEs in terms of grid data reduction approach at higher data densities (75% and 50%). (iii) LiDAR datasets can be reduced to 50% density level while still maintaining the DTM accuracy.

Due to advancements and improvements in instrumentation, software, processes, applications, and understanding, airborne LiDAR is one of the most capable, effective, and reliable alternative to traditional systems for gathering high-accuracy and high-density 3D terrain data leading to mapping products. The

limitations of the use of LiDAR data in constructing DTMs are the magnitude of data and the intense post-processing that can be required to transform raw LiDAR data into point clouds and eventually DTMs and other data products. However, high-density data associated with LiDAR lead to imposing challenges with respect to data storage, processing and manipulation. Large data volumes procured from LiDAR often require data reduction without losing relevant geometric details while constructing DTMs because the quality of LiDAR-derived DTMs equates to how well it represents the terrain undulation and continuity. Ultimately, the results of this study show that uniform algorithm is favoured for data reduction due to its lowest RMSEs and MAEs. The identification of terrain feature points is important because all data points do not contribute optimally to the DTM accuracy. Therefore, the data should be reduced by keeping critical data (considering terrain features). Due to the required DTM accuracy, extensive attention should be paid to reducing LiDAR data without extraction critical terrain elements. In order to represent the terrain morphology with the reduced data, further studies using diverse data reduction algorithms for smaller data density intervals (in relation to landform types) are necessary to determine the effective data reduction algorithm and the threshold data density for constructing DTMs.

ACKNOWLEDGEMENTS

This study was supported by Afyon Kocatepe University Scientific Research Projects Coordination Department (Project No: 16.KARIYER.87).

REFERENCES

Aguilar, F.J., Agüera, F., Aguilar, M.A., Carvajal, F. 2005. Effects of terrain morphology, sampling density and interpolation methods on grid DEM accuracy. *Photogrammetric Engineering and Remote Sensing*, 71 (7), 805-816.

Aguilar, F.J., Aguilar, M.A., Agüera, F., 2007. Accuracy assessment of digital elevation models using a non-parametric approach. *International Journal of Geographical Information Science*, 21 (6), 66-686.

Aguilar, F.J., Mills, J.P. 2008. Accuracy assessment of LiDAR-derived digital elevation models. *The Photogrammetric Record*, 23 (122), 148-169.

Anderson, E.S., Thompson, J.A., Austin, R.E. 2005 LIDAR density and linear interpolator effects on elevation estimates. *International Journal of Remote Sensing*, 26 (18), 3889-3900.

Anderson, E.S., Thompson, J.A., Crouse, D.A., Austin, R.E. 2006. Horizontal resolution and data density effects on remotely sensed LIDAR-based DEM. *Geoderma*, 132 406– 415.

Arab-Sedze, M., Heggy, E., Bretar, F., Berveiller, D., Jacquemoud, S. 2014. Quantification of L-band InSAR coherence over volcanic areas using LiDAR and in situ measurements. *Remote Sensing of Environment*, 152, 202-216.

Arun, P.V. 2013. A comparative analysis of different DEM interpolation methods. *The Egyptian Journal of Remote Sensing and Space Sciences*, 16, 133-139.

Cavalli, M., Tarolli, P. 2011. Application of LiDAR technology for rivers analysis. *Italian Journal of Engineering Geology and Environment*, Special Issue (1), 33-44.

Chaplot, V., Darboux, F., Bourennane, H., Leguédois, S., Silvera, N., Phachomphon, K. 2006. Accuracy of interpolation techniques for the derivation of digital elevation models in relation to landform types and data density. *Geomorphology*, 77, 126-141.

Chen, C.F., Yue, T.X. 2010. A method of DEM construction and related error analysis. *Computers and Geosciences*, 36 (6), 717-725.

Chu, H.J., Chen, R.A., Tseng, Y.H., Wang, C.K. 2014. Identifying LiDAR sample uncertainty on terrain features from DEM simulation, *Geomorphology*, 204, 325-333.

Cressie, N.A.C. 1991. Statistics for Spatial Data. New York: John Wiley and Sons.

Dorn, H., Vetter, M., Höfle, B. 2014. GIS-based roughness derivation for flood simulations: a comparison of orthophotos, LiDAR and crowdsourced geodata. *Remote Sensing*, 6, 1739-1759.

Erdogan, S. 2010. Modelling the spatial distribution of DEM error with geographically weighted regression: an experimental study. *Computers and Geosciences*, 36, 34-43.

Fassnacht, F.E., Hartig, F., Latifi, H., Berger, C., Hernández, J., Corvalán, P., Koch, B. 2014. Importance of sample size, data type and prediction method for remote sensing-based estimations of aboveground forest biomass. *Remote Sensing of Environment*, 154, 102-114.

Fisher, P.F., Tate, N.J. 2006. Causes and consequences of error in digital elevation models. *Progress in Physical Geography*, 30 (4), 467-489.

Garnero, G., Godone, D. 2013. Comparisons between different interpolation techniques. *International Archives of the Photogrammetry, Remote Sensing and Spatial Information Sciences*. XL-5/W3, 139-144.

Geomagic Support Center 2014. Overview of the Point Sampling Commands. <support1.geomagic.com>

Gong, J., Li, Z., Zhu, Q., Sui, H., Zhou, Y. 2000. Effects of various factors on the accuracy of DEMs: an intensive experimental investigation. *Photogrammetric Engineering and Remote Sensing*, 66 (9), 1113-1117.

Gumus, K., Sen, A. 2013. Comparison of spatial interpolation methods and multi-layer neural networks for different point distributions on a digital elevation model. *Geodetski Vesnik*, 57 (3), 523-543.

Heckbert, P., Garland, M. 1997. Survey of polygonal surface simplification algorithms. *Proceedings of the 24th Annual Conference on Computer Graphics and Interactive Techniques*, SIGGRAPH ´97, pp. 209-216.

Hodgson, M.E., Bresnahan, P. 2004. Accuracy of airborne LiDAR-derived elevation: empirical assessment and error budget. *Photogrammetric Engineering & Remote Sensing*, 70 (3), 331-339.

Immelman J., Scheepers L.G.C. 2011. The effects of data reduction on LiDAR-based digital elevation models, *4th International Congress on Image and Signal Processing*, Shanghai, China, 1694-1698.

Joseph, V.R. 2006. Limit Kriging. *Technometrics*, 48 (4), 458-466.

Kraus, K., Mikhail, E. 1972. Linear least squares interpolation. *Photogrammetric Engineering*, 38, 1016-1029.

Krige, D.G. 1951. A statistical approach to some basic mine valuation problems on the Witwatersrand. *Journal of the Chemical, Metallurgical and Mining Society of South Africa*, 52 (6), 119-139.

Krivoruchko, K., Gotway, C.A. 2004. Creating exposure maps using Kriging. *Public Health GIS News and Information*, 56, 11-16.

Lee, K.H., Woo, H., Suk, T. 2001. Point data reduction using 3D grids. *The International Journal of Advanced Manufacturing Technology*, 18 (3), 201-210.

Li, Z., Zhu, C., Gold, C. 2005. Digital Terrain Modeling: Principles and Methodology. Boca Raton: CRC Press.

Liu, X., Zhang, Z., Peterson, J., Chandra, S. 2007. The effect of LiDAR data density on DEM accuracy. *International Congress on Modelling and Simulation: Land, Water and Environmental Management: Integrated Systems for Sustainability*, Christchurch, New Zealand, 10-13 December 2007, pp. 1363-1369.

Liu, X. 2008. Airborne LiDAR for DEM generation: some critical issues. *Progress in Physical Geography*, 31 (1), 31-49.

Liu, X., Zhang, Z. 2008. LiDAR data reduction for efficient and high quality DEM generation, The International Archives of the Photogrammtery, *Remote Sensing and Spatial Information Sciences*, XXXVII, 173-178.

Liu, H., Kiesel, J., Hörmann, G., Fohrer, N. 2011. Effects of DEM horizontal resolution and methods on calculating the slope length factor in gently rolling landscapes. *Catena*, 87 (3), 368-375.

Ma, R., Meyer, W. 2005. DTM generation and building detection from LiDAR data. *Photogrammetric Engineering and Remote Sensing*, 71, 847-854.

Maune, D.F., Kopp, S.M., Crawford, .A., Zervas, C.E. 2007. Introduction. In D.F. Maune (Ed.), *Digital Elevation Model Technologies and Applications: The DEM Users Manual* (2nd ed.) (pp. 1-36). Bethesda: American Society for Photogrammetry and Remote Sensing.

Maune, D.F. 2008. Aerial mapping and surveying. In S.O. Dewberry, and L.N. Rauenzahn (Eds.), *Land Development Handbook* (3rd ed.) (pp. 877-910). New York: McGraw-Hill.

Mount St. Helens LiDAR Data 2006. <https://wagda.lib.washington.edu/data/type/elevation/lidar/st_helens/>

Mukherjee, S., Joshi, P.K., Mukherjee, S., Ghosh, A., Garg, R.D., Mukhopadhyay, A. 2013. Evaluation of vertical accuracy of open source digital elevation model (DEM). *International Journal of Applied Earth Observation and Geoinformation*, 21, 205-217.

Polat, N., Uysal, M. 2015. Investigating performance of Airborne LiDAR data filtering algorithms for DTM generation. *Measurement*, 63, 61-68.

Rayburg, S., Thoms, M., Neave, M. 2009. A comparison of digital elevation models generated from different data sources. *Geomorphology*, 106, 261-270.

Razak, K.A., Straatsma, M.W., van Westen, C.J., Malet, J.P., de Jong, S.M. 2011. Airborne laser scanning of forested landslides characterization: Terrain model quality and visualization. *Geomorphology*, 126, 186-200.

Renslow, M.S. 2012. Introduction. In M.S. Renslow (Ed.), *Manual of Airborne Topographic LiDAR* (pp. 1-5). Bethesda: ASPRS.

Sailer, R., Rutzinger, M., Rieg, L. Wichmann, V. 2014. Digital elevation models derived from airborne laser scanning point clouds: appropriate spatial resolutions for multi-temporal characterization and quantification of geomorphological processes. *Earth Surface Processes and Landforms*, 39 (2), 272-284.

Tan, Q., Xu, X. 2014. Comparative analysis of spatial interpolation methods: an experimental study. *Sensors and Transducers*, 165 (2), 155-163.

Tarolli, P., Arrowsmith, J.R., Vivoni, E.R. 2009. Understanding earth surface processes from remotely sensed digital terrain models. *Geomorphology*, 113, 1-3.

Vianello, A., Cavalli, M., Tarolli, P. 2009. LiDAR-derived slopes for headwater channel network analysis. *Catena*, 76 (2), 97-106.

Wehr, A., Lohr, U. 1999. Airborne laser scanning-An introduction and overview. *ISPRS Journal of Photogrammetry and Remote Sensing*, 54, 68-82.

Weng, Q. 2006. An evaluation of spatial interpolation accuracy of elevation data. In A. Riedl, W. Kainz, and G.A. Elmes (Eds.), *Progress in Spatial Data Handling* (pp. 805-824). Berlin: Springer-Verlag.

Yan, W.Y., Shaker, A., El-Ashmawy, N. 2015. Urban land cover classification using airborne LiDAR data: A review. *Remote Sensing of Environment*, 158, 295-310.

Yilmaz, M., Gullu, M. 2014. A comparative study for the estimation of geodetic point velocity by artificial neural networks. *Journal of Earth System Sciences*, 123 (4), 791-808.

International Journal of Engineering and Geosciences (IJEG),
Vol;2, Issue;01, pp. 17-26, February, 2017, ISSN 2548-0960, Turkey,
DOI: 10.26833/ijeg.286691

OPEN GEOSPATIAL CONSORTIUM WEB MAP AND FEATURE SERVICES AND FREE/OPEN SOURCE SERVER/CLIENT SOFTWARES

Varol, M.., [1]* Sanlıoglu, I.,[2]

[1]General Command of Mapping, Cebeci, Ankara, (mesud.varol@gmail.com)

[2]Assist.Prof. Dr., Selçuk University, Geomatics Engineering, Konya, (sanlioglu@selcuk.edu.tr)

*Corresponding Author, Received: 20/01/2017, Accepted: 31/01/2017

ABSTRACT: Usage of geospatial data enables decisions to be more effective and stronger in critical fields. Since geospatial data is very expensive source and the most time-consuming step, mostly it is not possible to find the required data ready to use. Therefore different projects have been developed and tried to implement by several countries to keep geospatial data which is required to collect and managed, accessible and usable. At this study Open Geospatial Consortium standarts were explained, the focus was given on WFS and WMS because of their increasing popularity. Concurrently free and/or open source WMS/WFS server and client softwares were investigated.

Keywords: *Interoperability, Standards, Open Geospatial Consortium, Web Map Sevice, Web Feature Service, Open Source Softwares.*

1. INTRODUCTION

Gathering, compiling, presenting and analyzing of the information is one of the most sought-after topics to be explored today. If the positional characteristic of the knowledge that many disciplines need in common also belongs to the account, the degree of complexity will increase in the same way. It is also important that the information which is no doubt about its authenticity and proven knowledge needs to be communicated to the right place at the right time, fast and up-to-date. Developments in computer technology have increased the feasibility of issues such as data storage, data organizing, data sharing, re-evaluation of data, data analysis and the best representation of the earth's surface. The diversity of applications has increased as the importance of geographical information systems has increased and many disciplines have begun to benefit from this technology. The variety of applications and the geographic data structures used in applications has created the needs to regulate interoperability, data and application standards. For this purpose, the international standards used in the internet based geographical information systems have been examined and the developed application has been ensured to conform to the mentioned standards.

In the first part of the done work, the definition of interoperability, its importance and the stages in which it can be carried out today, the advantages of these standards and the aims of their development are explained from the standards established to enable interoperability. In the second part, OGC standards are discussed. In the third part, WMS and WFS, which are frequently used OGC standards, are discussed in more detail. The fourth section introduces open source software that will allow the server to be installed and then be used by the client to view the data. In the last section, the facilities provided by WFS for data presentation are mentioned in terms of interoperability and evaluated in terms of geomatics engineering.

2. INTEROPERABILITY AND FUNDAMENTAL CONCEPTS

In order to fully understand and use the capabilities and benefits of information system technologies, the data must be shared between different users, and the interoperability of the systems must also be ensured.

The broadest definition of interoperability, which can be described as the ability of information to be used and transferred between institutions and information systems, is effective information sharing (Anonim, 2012).

Interoperability; is also referred as "the ability of a system or process to use its knowledge and / or functions of another system or process within the framework of common standards" (Europa, 2016).

Interoperability needs can be examined in three dimensions as technical, organizational and semantic. At technical level, the organizational dimension is based on engineering methodologies such as process modeling languages, object oriented software engineering, rather than technology, while focusing on the technologies that enable information sharing among different applications. Within the scope of organizational interoperability, the business processes of the institutions are dealt with by modeling them in relation to the other related institutions and the business processes formed in order to provide the integration between the aims of the institutions and the applications and systems that form the technical infrastructure, in other words, to exchange the shared information more effectively and institutional structuring is targeted. It also includes processes such as re-engineering, workflow management within the organization and between institutions, and identification of needs for processes and services. In the context of meaningful interoperability, there are studies to be understood and interpreted correctly by institutions outside the institution that produces it.

There are needs to establish standards that can be applied to make interoperability possible and to use these standards.

Standards-compliant interfaces need to be created to share data. However, in addition to this compatibility, modeling, naming and identification of data and preparation of metadata forms need to be carried out in coordination. In this respect, studies are being continued in many countries and standards are being prepared by international organizations. OGC and ISO / TC 211 Geographic Information / Geomatics working groups, which have been operating since 1994, are at the top of these organizations. Their main purpose is to ensure that the geoprocessing services and the geographic data are in a certain standard. Thus establishing global international standards to ensure data exchange and interoperability (Anonim, 2016 - ISO/TC, 2016).

In addition to these organizations, there are also DGIWG (Defense Geospatial Information Working Group), INSPIRE organizations.

The common aim of all these organizations is,

- Increasing access to quality geospatial data,
- Increasing the availability of current geospatial data,
- Increasing the understandability of the existing geospatial data,
- To increase the effective and economical use of geospatial data,
- Providing a common solution to the problems,
- Providing software and hardware compatibility,
- Reduction of inefficiency in the collection, storage, processing and distribution of spatial data.

3. OGC

OGC is an international service providing co-operation in geographical and location based studies. OGC is an international industry consortium of over 521 companies, government agencies and universities participating in a consensus process to develop publicly available interface standards.

Latterly, with the use of the internet environment for geospatial data sharing, geographical web services has emerged. For this purpose, OGC especially aims to standardize geospatial web services by making standards and disseminate usage, and to provide interoperability for GIS (Emem O., 2007).

The mission of the OGC is to promote the development and use of advanced open systems standards and techniques in the area of geoprocessing and related information technologies. OGC's goal is to provide interoperable solutions for geographic information communities. The OGC is also known as the Open Geospatial Interoperability Specifications Consortium (OpenGIS) consortium.

As a result of OGC's ongoing studies, it is possible to use WFS, WMS, Geography Markup Language (GML), OGC Keyhole Markup Language (KML), Web Coverage Service (WCS), Web Catalog Service (CS/W), Web Map Context (WMC), Coordinate Transformation Service (CTS), Location Service and Web Registry Service (WRS).

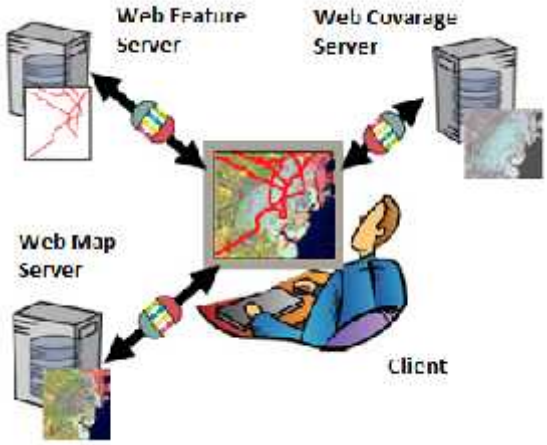

Figure 1. Server/Client schema

The OGC lists the benefits of establishing standards in the GIS field and the facilities that the generated data will have:

- Geospatial content should be easy to find, without regard to its physical location.
- Once found, geospatial content (and services) should be easy to access or acquire.
- Geospatial content from different sources should be easy to integrate, combine, or use in spatial analyses, even when sources contain dissimilar types of data (raster, vector, coverage, etc.) or data with disparate feature-name schemas.
- Geospatial content from different sources should be easy to register, superimpose, and render for display.
- Special displays and visualizations, for specific audiences and purposes, should be easy to generate, even when many sources and types of content are involved.
- It should be easy, without expensive integration efforts, to incorporate into enterprise information systems geoprocessing resources from many software and content providers (Kantar F., 2003).

OGC Web Service standards, which have a significant place in terms of web based geographic information systems are:

- Web Map Service (WMS)
- Web Feature Service (WFS)
- Web Coverage Service (WCS)
- Catalogue Service for the Web (CS/W)
- Web Coordinate Transformation Service (WCTS)
- Geography Markup Language (GML)
- Filter Encoding Implementation Specifaction (FES)
- Gazetteer Service Profile (WFS – G)
- Web Map Tile Service - WMTS
- Web Map Context (WMC)
- Web Coverage Processing Service (WCPS)
- Coordinate Transformation Service (CTS)
- Geospatial eXtensible Access Control Markup Language (GeoXACML)
- Keyhole Markup Language (KML)
- Table Joining Service (TJS)

4. WEB MAP SERVICE – WMS

By far the most popular and widely implemented of the geospatial standards, the OGC Web Map Service (WMS versions 1.1.1 and 1.3; ISO 19128) supports the request and display of maps derived from data accessed by the service. Maps, delivered as graphical images (GIF, JPEG, TIFF, etc.), may be requested from one or more WMSs overlaid in browsers or client applications. Features "behind" the map can also be queried, and their properties can be returned to a requesting client (Nebert D., 2007).

Schemas for validating the "capabilities" of an XML file returned from a WMS service exist, and compliance testing is available through the OGC for assessing WMS performance on all key functionalities.

WMS version 1.1.1 is the most widely deployed (ISO 19128, however, is harmonized with WMS version 1.3 but is not yet widely deployed) and is recommended for inclusion in the SDI 1.0 standards suite (Nebert D., 2007). The Geographic Data Infrastructure mentioned here is a project that is aimed at establishing the standards required for the systems used to gain the ability to use the knowledge and/or functions of another system within the framework of common standards (KYM-75, 2016).

The WMS specification standardizes simple query operations such as client requesting maps over the Internet, presenting data to servers, and displaying coordinates and attributes of requests. OGC first released the version 1.0.0 of WMS specification in 2000. After the release of the first version, the current version 1.3.0 was released in 2004 (Emem O., 2007). WMS is an international application standard published as ISO 19128 (Web Map Server Interface) standard, which was adopted by ISO in 2005 as it is OGC specification. The WMS specification defines a number of request types, and for each of them a set of query parameters and associated behaviors. A WMS-compliant server must be able to handle at least the following 2 types of WMS requests:

- GetCapabilities: is used to obtain the service metadata and accepted request parameters. Returns an XML document with metadata of the Web Map Server's information
- GetMap: is used to obtain the coordinate spatial data image. Returns an image of a map according to the user's needs.

And support for the following types is optional:

- GetFeatureInfo: A function that provides attributes for a specific detail shown in the map. Returns info about feature at a query location.
- DescribeLayer: A function that provides access to additional information about WFS and WCS layers. Returns an XML description of one or more map layers.
- GetLegendGraphic: A function that allows access to the legend created for the map. Returns a legend image (icon) for the requested layer, with label(s).

Performing mandatory and optional functions from WMS using a standard web browser is possible by requesting in URL form. The client first needs to get GetCapabilities and get the data and related parameters on the server. As a result of the GetCapabilities request, the server sends an XML file containing the necessary information (Figure 2).

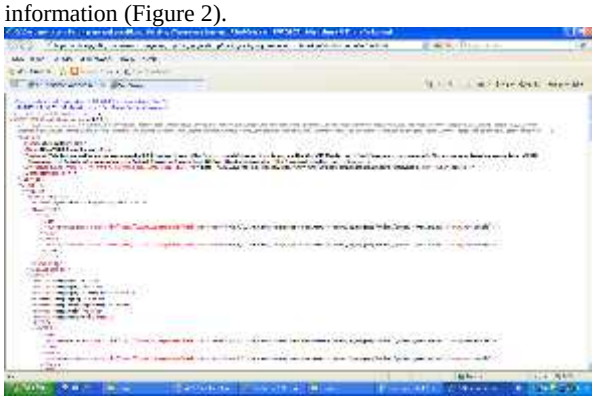

Figure 2. GetCapabilities request response

When performing a GetMap request, the client can determine the information that wants to appear on the map. A standard web browser with URL-formatted GetMap request from WMS example could look like as follows:

```
http://localhost/cgi-bin/mapserv.exe?
map=/ms4w/apps/ms_turkiye/service/config.map
&version=1.1.1&service=WMS
&request=GetMap
&srs=EPSG:4326
&bbox=-180,-90,180,90
&format=image/png
&layers=land_shallow_topo_2048,nehirler
&styles=,
&transparent=true
&width=500&height=300
```

As a result of this request, the server from the server will return a two-layered png format image (Figure 3).

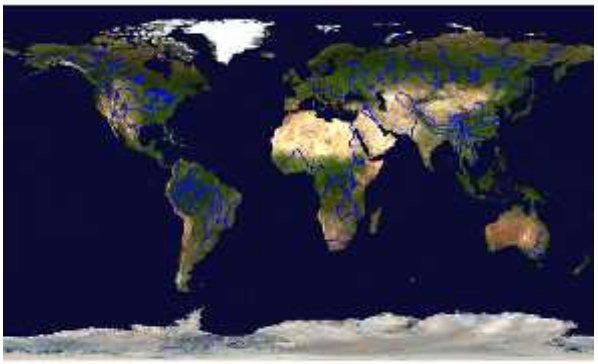

Figure 3. WMS GetMap request response

The commands used in the request are described in Table 1.

Table 1. Commands and functions in GetMap request line

Command	**Function**
Map	The root layer in the WMS context corresponds to the whole mapfile.
Service	The service used is specified.
Version	Request version.
Request	Request name (GetMap).
Srs	Spatial Reference System.
Format	Output format of map.
Bbox	Bounding box corners (lower left, upper right) in SRS units.
Layers	Comma-separated list of one or more map layers. Optional if SLD parameter is present.
Transparent	Transparency/Opacity is specified.
Width	Width in pixels of map picture.
Height	Height in pixels of map picture.

GetFeatureInfo is an optional function. Not all WMS servers can answer this request. The GetFeatureInfo operation requests the spatial and attribute data for the features at a given location on a map (Figure 4). In this case, the client queries the image and sends the coordinate information and layer of detail to the server (Emem O., 2007).

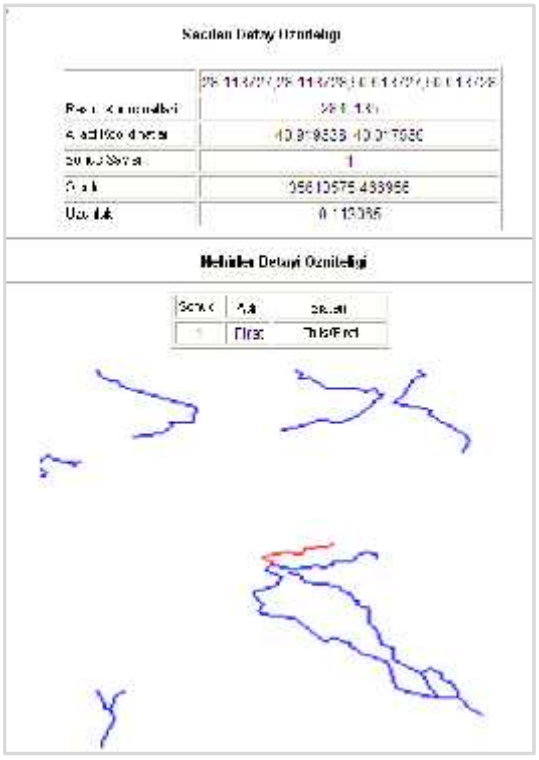

Figure 4. WMS GetFeature request response

WMS has been identified in two types in the OGC document. These are basic WMS and Cascading Map Server. Basic WMS supports the basic functions listed above. The Cascading Server behaves like a client of another WMS and can aggregate images from different servers into a service. It also supports format and coordinate conversions (Emem O., 2007).

5. WEB FEATURE SERVICE – WFS

The OGC Web Feature Service (WFS), takes the next logical step of by defining interfaces for data access and manipulation operations on geographic features using HTTP as the distributed computing platform. As it is known WMS interface return only an image, which end-users cannot edit or spatially analyze.

Via these interfaces, a web user or service can combine, use and manage geodata -the feature information behind a map image- from different sources by invoking the following WFS operations on geographic features and elements:

- Create a new feature instance,
- Delete a feature instance,
- Update a feature instance,
- Lock a feature instance,
- Get or query features based on spatial and non-spatial constraints (Open Geospatial Consortium, 2017b).

In this context, WFS; the client generates the request and posts it to a web feature server, the request naturally requests a data transfer from the server or a query on the data held in the server returns the desired result.

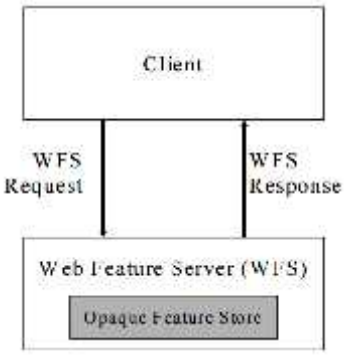

Figure 5. Web Feature Service Client/Server Schema

Requests are generated by the client computer in the direction of the user's request as specified in the WFS standard and are requested from the server with the help of the widely used HTTP protocol. The WFS server examines incoming requests, evaluates the request if the arrived WFS request is appropriate, and sends the final result to the client computer in a format that conforms to the WFS standard. When the WFS has completed processing the request, a query result is generated by either compiling the vector data or the vector data (Figure 5).

After this simple identification, the OGC WFS service service can be further elaborated. The OGC WFS service uses GML (Geography Markup Language) to transfer data and query results. Therefore, the data transferred from the server and sent to the server must be kept absolutely in the GML structure. These transfers do not use industry standard or other popular vector data formats. The GML structure allows a client to request more than one service, and allows a server to serve more than one client. The minimum requirements for a typical WFS service can be listed as follows:

- The Interfaces must be defined in XML (Extensible Markup Language).
- GML must be used to express features within the interface.
- At a minimum a WFS must be able to present features using GML.
- The predicate or filter language will be defined in XML and be derived from CQL as defined in the OpenGIS Catalogue Interface Implementation Specification.
- The datastore used to store geographic features should be opaque to client applications and their only view of the data should be through the WFS interface.

5.1. WFS Operations

The details of the GetCapabilities, DescribeFeatureType and GetFeature functions from the Basic WFS functions and Transaction and LockFeature functions mentioned above are as follows.

5.1.1. GetCapabilities

A web feature service must be able to describe its capabilities. Specifically, it must indicate which feature types it can service and what operations are supported on each feature type.

5.1.2. DescribeFeatureType

With this operation, the structure of the vector data presented on the server can be queried. Upon request, it provides information on the structure of any detail type. For example; the feature attribute and geometry's detail is acquired by this capability.

5.1.3. GetFeature

This function allows the client to specify what properties the server wants and what data it wants. So it brings back specimen instances. For example; The server can be queried about Turkey's provinces districts in the Mediterranean Region which have population more than 50.000.

5.1.4. Transaction

Through this function, the operation performed on the data is defined. These operations can be generally classified as adding data, changing or deleting the existing data.

5.1.5. LockFeature

This function is very important, it allows one or more copies of the processed data to be locked and stored. A LockFeature operation provides a long-term feature locking mechanism to ensure consistency in edit transactions. If one client fetches a feature and makes some changes before submitting it back to the WFS, locks prevent other clients from making any changes to the same feature, ensuring a transaction that can be serialized. If a WFS server supports this operation, it will be reported in the server's GetCapabilities response.

6. FREE/OPEN SOURCE SERVER/CLIENT SOFTWARES

6.1. Server Softwares

6.1.1. MapServer For Windows

MapServer is an Open Source platform for publishing spatial data and interactive mapping applications to the web. Originally developed in the mid-1990's at the University of Minnesota, MapServer is released under an MIT-style license, and runs on all major platforms (Windows, Linux, Mac OS X). All source code is openly available via GitHub.

The biggest advantage of MapServer software is that it supports many OGC standards. While most open source software supports OGC WMS, WFS, WCS, GML standards, MapServer supports OGC WMC, Styled Layer Descriptor –SLD, Sensor Observation Service – SOS, Observations and Measurements – OM, Sensor Web Enablement - SWE standards as well.

- Advanced cartographic output
  - Scale dependent feature drawing and application execution
  - Feature labeling including label collision mediation
  - Fully customizable, template driven output
  - TrueType fonts
  - Map element automation (scalebar, reference map, and legend)
  - Thematic mapping using logical- or regular expression-based classes
- Support for popular scripting and development environments
  - PHP, Python, Perl, Ruby, Java, and .NET
- A multitude of raster and vector data formats
  - TIFF/GeoTIFF, NetCDF, MrSID, ECW, and many others via GDAL
  - ESRI shapfiles, PostGIS, SpatiaLite, ESRI ArcSDE, Oracle Spatial, MySQL
- Map projection support
  - On-the-fly map projection with 1000s of projections through the PROJ.4 library

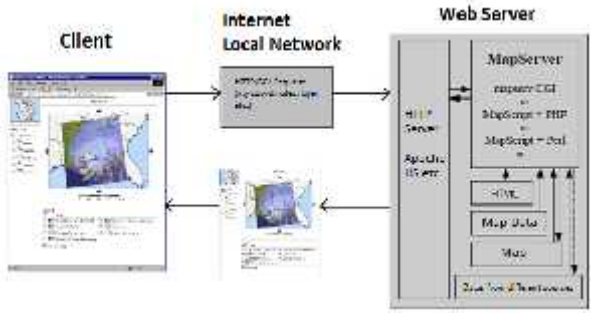

Figure 6. MapServer architecture

For more information visit http://www.mapserver.org.

6.1.2. GeoServer

GeoServer is a Java-based software server that allows users to view, share and edit geospatial data. GeoServer is free software. This significantly lowers the financial barrier to entry when compared to traditional GIS products. In addition, not only is it available free of charge, it is also open source. It is already implementing the WMS, WFS and WCS standarts. One of its main strength is the full implementation of the WFS-T protocol. The software supports JPEG, PNG, SVG, GIF, GeoJSON, PDF, GeoRSS, KML / KMZ, GML, Shapefile data formats used in GIS applications.

GeoServer can display data on any of the popular mapping applications such as Google Maps, Google Earth, Yahoo Maps, and Microsoft Virtual Earth. In addition, GeoServer can connect with traditional GIS architectures such as ESRI ArcGIS.

Other geographic data can easily adapt to Geoserver. It is a free software that can work with PostGIS, Oracle Spatial, ArcSDE, DB2, MySQL, Shapefile, GeoTIFF, ECW environments as data source. Geoserver architecture is as shown in Figure 7.

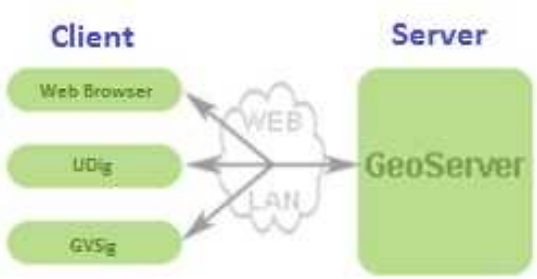

Figure 7. Geoserver architecture

For more information visit http://geoserver.org/.

6.2. Client Softwares

6.2.1. Cesium

Cesium is an open-source JavaScript library for world-class 3D globes and maps. Cesium was founded by Analytical Graphics, Inc. (AGI) in 2011 as a cross-platform virtual globe for dynamic-data visualization in the space and defense industries. With Cesium, the newest web-based virtual globe application, users have the ability to view spatial data independently of the operating system. OGC WMS, WMTS, CityGML, KML standards are supported.

Cesium;

- Multiple view modes include 2D, 3D and 2.5D Columbus view,
- Stand-alone or local network operations,
- Three-dimensional display no need to install any extension,
- Runs on Windows, Linux, and Mac operating systems,
- There are many features such as dynamic time data display without writing any code.
- Supports visualizing 3D models using gITF

Figure 8. An overview of Cesium

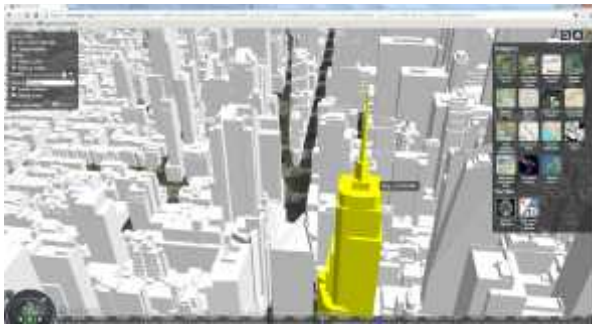

Figure 9. 3D tiles from Cesium

For more information visit http://cesiumjs.org/.

6.2.2. ArcGIS Explorer

ArcGIS Explorer is a free viewer software developed by ESRI (Figure 10). With this software;

- Datas can be viewed in Shapefile, KML / KMZ, GPX and raster formats (JPEG 2000, GeoTIFF, MrSID),
- Access to mapping services ArcGIS for Server; ArcIMS; and OGC WMS, and GeoRSS feeds.
- In addition to the maps provided by ArcGIS Online as base images, different sources can be used.
- View maps and globes in any projection or coordinate system.

One of the biggest advantages of the software is that the data can be displayed in both two and three dimensions.

It is also possible for users to develop and add additional tools with free downloadable software development kit (SDK). Users able to access different abilities from ESRI users forums by integrating the extensions that different users have developed.

And different languages are supported on the application (English, French, Japanese, Chinese, German, or Spanish).

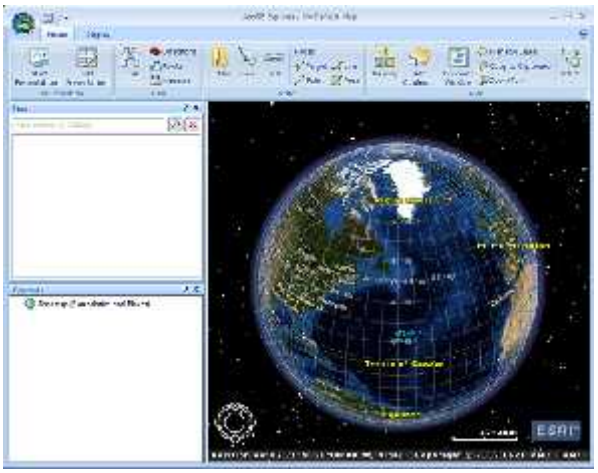

Figure 10. ArcGIS Explorer screen capture

For more information visit http://www.esri.com/software/ arcgis/explorer-desktop.

6.2.3. Gaia

Gaia is a platform designed for advanced geospatial network and SDI needs. Based on the CarbonTools PRO open-geospatial development toolkit, this viewer can access an array of geospatial sources such as the OGC WMS, WMTS, WCS, WFS, and FES, services such as Microsoft Bing Maps, Yahoo! Maps and OpenStreetMap (OSM), as well as file formats such as ESRI Shapefiles, Google Earth KML/KMZ, DXF, MIF, GML and GML Simple Features (GMLsf).

With Gaia users can use geospatial content from different sources and overlay them into a single map view, with each layer individually configured and styled. The Gaia multi-layer view allows seamless use of multiple layers of different types. Panning, zooming and other mapping tools provide a fast and convenient tool for browsing the map. Gaia uses dynamic caching of content to memory, providing enhanced mapping performance.

Gaia includes an open API to allow developers to modify and enhance the application. Gaia makes it easy to create meaningful maps, and includes tools to create your own map symbols. Gaia can run on any compliant Linux and Mac OS platforms.

Şekil 11. Gaia screen capture

For more information visit http://www.thecarbonproject.com/ Products/Gaia.

6.2.4. OpenLayers

OpenLayers, another open source client software, makes it easy to put a dynamic map in any web page. It can display map tiles, vector data and markers loaded from any source. OpenLayers has been developed to further the use of geographic information of all kinds. It is completely free, Open Source JavaScript, released under the 2-clause BSD License (also known as the FreeBSD).

With OpenLayers;

- Many map controls will arrive ready for their abilities,
- Render vector data from GeoJSON, TopoJSON, KML, GML, Mapbox vector tiles, and other formats,
- Leverage Canvas 2D, WebGL, and all the latest greatness from HTML5,
- Pull tiles from OSM, Bing, MapBox, Stamen, and any other source. OGC WMS, WFS and untiled layers also supported.
- It will benefit from many user experiences by reaching large participating user forums.

It is easier to integrate GeoServer users with OpenLayers. Figure 13 shows a WFS image of Openlayers.

Figure 13. WFS image of Openlayers

For more information visit https://openlayers.org/.

6.2.5. QGIS

QGIS is an Open Source Geographic Information System client application. QGIS currently runs on most Unix platforms, Windows, and OS X. QGIS is developed using the Qt toolkit and C++.

The software supports Shapefile, GeoDatabase, MapInfo, Microstation, DXF, MsSQL database formats. Spatially-enabled tables and views using PostGIS, SpatiaLite and MS SQL Spatial, Oracle Spatial, vector formats supported by the installed OGR library, including ESRI shapefiles, MapInfo, SDTS, GML and many more. Online spatial data served as OGC Web Services, including WMS, WMTS, WCS, WFS, and WFS-T. Raster and imagery formats supported by the installed GDAL (Geospatial Data Abstraction Library) library, such as GeoTIFF, ERDAS IMG, ArcInfo ASCII GRID, JPEG, PNG and many more.

With QGIS;

- Quick view of layers served from different sources,
- Easy-to-use tools,
- Supported 2700 known coordinate systems and user defined coordinate system support,
- Extension support for many analyzes,
- Raster image analysis,
- Possibility of three dimensional display with Qgis2threejs plugin,
- Temporal data display with TimeManager plugin,
- Able to apply topology rules.

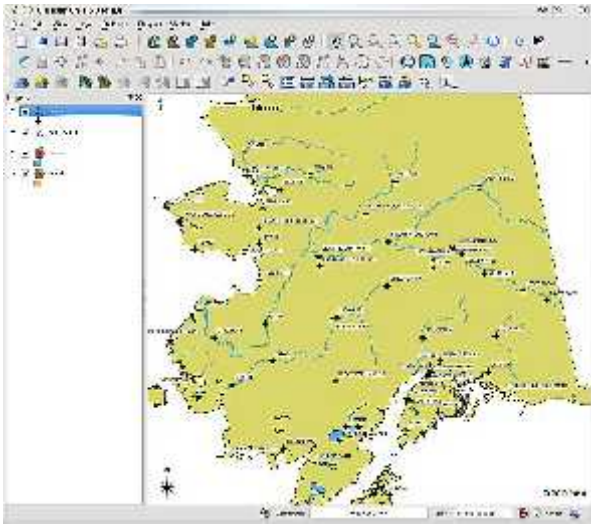

Figure 14. QGIS screen capture

For more information visit http://www.qgis.org.

6.2.6. GvSIG

GvSIG is an open source geographic information client software designed to manage geospatial data (Figure 15). It is easy to work in a variety of formats with gvSIG Desktop, vector and raster files, databases and remote services. GvSIG supports OGC WMS, WFS, WCS, WFS-T and WPS standards. GvSIG can access PostGIS, MySQL, ArcSDE, Oracle, JDBC, and CSV databases.

The possibilities provided by GvSIG software;

- Standard GIS tools (zoom in, zoom out, etc.)
- Query with SQL statement,
- Three-dimensional imaging,
- Applying topology rules,
- Raster and vector data analysis,
- Mobile application support.

Figure 15. GVSIG scree capture

For more information visit http://www.gvsig.com.

7. CONCLUSION AND RECOMMENDATIONS

Today, the importance of communication and information sharing is increasing rapidly. As a consequence of the fact that most of the data used in the studies are spatial data, the importance of sharing these data with other institutions that need it has emerged. OGC standards play important role in sharing these data according to the principle of interoperability.

In the study, applications that support the OGC web services standards has been examined in the serve and view of vector and raster data. Free and open source software that are under review will also support Individuals/institutions/businesses beyond the budgetary obstacles they face when collecting and serving spatial data. You'll appreciate the ability to be able to freely experiment with technologies without paying any royalties, if you're starting a small company, a private venture, or even a project within a large company.

Publishing of data from any major spatial data source with free/open source software platforms and using OGC standards will serve all users who need the same data. By sharing the spatial data, repeated data collection is prevented and data collection costs will be reduced. By means of the standards, the data obtained from different sources can be easily coordinated, edged and served as images. When your data is kept in open formats, converting from one data type to another is straight forward, and there is probably a piece of software that does exactly that. Custom projects or analyses for specific purposes and users can be easily created and visual presentations are predicted to become feasible. Integration of spatial data from different softwares and data providers could be done without extra software, hardware and geographic transaction costs.

ACKNOWLEDGEMENTS

This study is derived from the postgraduate thesis that prepared by Eng.Mesud Behlül VAROL who is studying at Selcuk University Institute of Natural Science - Geomatics Engineering Department.

REFERENCES

Alameh N., 2010, OGC Web Services TestbedOWS-7, AIXM/WXXM Conference Washington DC

Anonim, 2012. E-dönüşüm Türkiye Projesi Birlikte Çalışabilirlik Esasları Rehberi Sürüm 2.1

Anonim, 2016. ISO/TC 211- 1, 2001, ISO 19101 Reference Model, ISO Standartları

AtlasStyler , http://www.geopublishing.org/gp_stable/as.jnlp [Accessed 06 May 2016]

ArcGIS Explorer, http://www.esri.com/software/arcgis/explorer/index.html [Accessed 19 Apr 2016]

Emem O., 2007. Mekânsal Veri ve Bilgi Altyapısının Uygulamalı Olarak Geliştirilmesi adlı Doktora Tez Çalışması Bildirisi, KTÜ

Europa, http://ec.europa.eu/idabc/en/document/2319/5644 .html [Accessed 21 Apr 2016]

Gaia Geospatial Platform, http://www.thecarbonproject.com/ Products/Gaia [Accessed 03 May 2016]

GeoServer, http://geoserver.org [Accessed 19 Apr 2016]

GRASS GIS, http://grass.osgeo.org [Accessed 03 May 2016]

INSPIRE Internet Sitesi, http://inspire.jrc.ec.europa.eu [Accessed 06 Mar 2016]

ISO/TC 211 Web Site [Online], www.isotc211.org [Accessed 19 Apr 2016]

MapServer, http://mapserver.org [Accessed 19 Apr 2016]

Nebert D., Carl REED, Roland M. WAGNER, 2007, Proposal for a Spatial Data Infrastructure Standards Suite: SDI 1.0

Open Geospatial Consortium, 2017a. OGC, http://www.opengeospatial.org/ogc/faq#5 [Accessed 04 Jan 2017]

Open Geospatial Consortium, 2017b. Standarts, http://www.opengeospatial.org/standards/wfs [Accessed 05 Jan 2017]

Open Geospatial Consortium, 2016. OGC, http://www. opengeospatial.org [Accessed 05 Mar 2016]

OSGeo4W, http://trac.osgeo.org/osgeo4w [Accessed 19 Apr 2016]

OpenGIS, http://www.opengis.ch [Accessed 06 May 2016]

OpenLayers, http://openlayers.org [Accessed 03 May 2016]

Portal gvSIG, http://www.gvsig.com [Accessed 06 May 2016]

Türkiye Ulusal Coğrafi Bilgi Altyapısı Kurulumu Projesi(KYM-75) Fizibilite Etüdü Raporu, 2010. M. Osman ÖZDEMİR, http://www.turksatglobe.com.tr/Views/Projects/ Contents/Files/CbsA/B_010_SUNUM_TASLAK_STANDARTLAR_OO.pdf [Accessed 02 Mar 2016]

Quantum GIS, http://www.qgis.org [Accessed 03 May 2016]

uDig, http://udig.refractions.net/ [Accessed 06 May 2016]

Vretanos P. A.,WFS Implementation Specification, https://portal.opengeospatial.org/files/?artifact_id=7176 [Accessed 06 Mar 2016]

Web Map Tile Service, http://www.cubewerx.com/ technology/wmts/ [Accessed 06 Apr 2016]

International Journal of Engineering and Geosciences (IJEG),
Vol;2, Issue;01, pp. 27-34, February, 2017, ISSN 2548-0960, Turkey,
DOI: 10.26833/IJEG.286034

DETERMINATION OF TRANSPORTATION NETWORKS BASE ON THE OPTIMAL PUBLIC TRANSPORTATION POLICY USING SPATIAL AND NETWORK ANALYSIS METHODS: A CASE OF THE KONYA, TURKEY

Emra Sert[1], Nurullah Osmanli[1], Rezzan Eruc[1], Mevlut Uyan[2,*]

[1]Konya Metropolitan Municipality, Department of Urban Information System, Konya, Turkey,
(emrasert@gmail.com, osmanlinurullah@gmail.com, rezzaneruc@konya.bel.tr)

[2]Selcuk University, Directorate of Construction & Technical Works, Konya, Turkey,(email:muyan@selcuk.edu.tr)

*Corresponding Author, Received: 15/01/2017, Accepted: 25/01/2017

ABSTRACT: Public transportation planning is one of the most important parts of transportation planning and it provides sustainable development for cities. According to only demands of citizen's and decisions of city managers obstruct for public transportation planning also taking policy in the long time period. Citizen's demands and city manager's decisions important factors in transportation planning but the other important factors; city's and citizen's characteristic features. Relational structure to be determining between spatial and network analysis with these features, according to these situation necessary making transtportation policies. The purposes of this paper are to determinate of transportation networks base on the optimal public transportation polices using spatial and network analysis methods of an urbanized city: Konya, Turkey.

Keywords: *Network Analysis, Spatial Analysis, Transportation, Vehicle Routing Problem (VRP).*

1. INTRODUCTION

The spatial distribution of transportation networks has considerable implications on the economic and social development of a country. Therefore, it is a major political issue in many parts of the world (Bigotte, et al., 2010). Transportation planners in developing countries face a number of problems that require innovative solutions such as rapidly growing population, traffic congestion and pollution due to the increasing number of vehicles. Transportation sector is the second largest energy consumer sector after the industrial sector and accounts for 30% of the world's total energy (Geng, et al., 2013).

Public transportation in developed countries is a crucial part of the solution to the nation's economic, energy and environmental challenges. Public transportation offers many advantages over individual transport modes. It costs less to the community, needs less urban space, is less energy-intensive, pollutes less, is the safest mode, improves accessibility to jobs and offers mobility for all. Many cities have invested in recent years in the construction, expansion or modernization of public transportation which is rapid transit systems. This is partly in response to increased traffic congestion and to the need to reduce carbon emissions (Gutiérrez-Jarpa, et al., 2013).

Public transportation planning is one of the most important parts of transportation planning and it provides sustainable development for cities. Thus, providing convenient planning strategies in which the travel behaviors of users are well-modeled has become a primary issue due to the influence of public access to urban public transportation systems (Gulhan, et al., 2013). Without the use of spatial analysis capabilities, formed with only basic data transportation plans do not coincide with both cities plans and daily urban mobility. Evaluation of spatial analysis in terms of transportation; social, demographic, economic, road network and urban reinforcement distribution for the current and future factors is to be determined according to the importance degree of the classification.

New technologies such as geographic information systems (GIS) provide a valuable tool to study the spatial structure of the transportation networks. They take into account the spatial autocorrelation in data, to create mathematical models of spatial correlation structures commonly expressed by various models. By development of GIS, it has been increasingly used as an important spatial decision support system for transportation network analysis. A number of GIS methods and techniques have been proposed to evaluate transportation network. Public transportation planning has been discussed in many studies using GIS methods (Caulfield, et al., 2013; DiJoseph, Chien, 2013; Gutiérrez-Jarpa, et al., 2013; Kim, Schonfeld, 2013; Zhou, et al., 2013; Dorantes, et al., 2012; Martens, et al., 2012; Mishra, et al., 2012; Murphy, 2012; Neutens, et al., 2012; Timilsina, Dulal, 2011; Bigotte, et al. 2010; Sayyady, Eksioglu, 2010; Soh, et al., 2010; Yang, Ferreira, 2009).

The purposes of this paper are to determinate of transportation networks base on the optimal public transportation polices using spatial and network analysis methods of an urbanized city: Konya, Turkey. Firstly, "minibus transportation" was evaluated in terms of across the city and transportation policies was attempted to establish accordin to housing-accessibility relationship. Secondly, "bus transportation" was evaluated in terms of northern part of the city and transportation policies was attempted to establish accordin to housing-accessibility relationship. Finally, according to the results of oth studies, foresights have attempted to establish for public transportation policy.

Figure1. The geographical position of Konya Metropolitan Municipality's boundary.

2. Materials and Method

2.1.Study Area

The city of Konya is geographically situated between 36.5º-39.5º north latitudes and 31.5 º-34.5 º east longitudes. It is the largest province of Turkey. Konya city's area is 38,257 km^2 (Uyan, 2013). Public transport in study area (Borders of Konya Metropolitan Municipality) comprises a bus network, minibus network and rail systems to serve the more than one million inhabitants of the city spread over an area of 2100 km². Study area is shown in Fig. 1. In Konya, the current state of numerical distribution of public transportation services is shown in Table 1. The average number of daily passengers for the tram as 90,000 people has been identified. In the northern region of Konya, in terms of public transport infrastructure, use of tram and minibus lines are more intense. Buses and minibuses density is usually composed in the city center. Traffic density in the city center is seriously affected this mobility.

Table 1. Public transportation type by current situation in study area.

Transportation Type	Number of vehicles	Passenger capacity	Number of stations	Number of trips (Daily)	Total line length (km)
Tram	60	532	35	285	21
Bus	310	308	1848	2037	1410
Minibus	530	17	198	411	751

2.2. Methodology

2.2.1. Data collection

Data for this study were acquired from the Social texture map database of the Konya Metropolitan Municipality. Social texture maps provide population, disabled, public transportation needs, working population and vehicleowning density maps (Fig. 2). Social texture maps carried out survey studies to determine the opinions of the citizens. Within the context of GIS to create the fundamental basis of the project, it was organized a survey covering all households in Konya. According to the results, the direct and cross-analysis was performed, and this data is used in many social projects. Frequency of social texture maps was modeled using the kernel density estimator (KDE) calculated in the Spatial Analyst extension of ArcGIS, version 10.0.

KDE are flexible, non-parametric methods and calculates the density of events the overall number of observations within a particular search radius from a target location (Kuo, et al., 2013; Harris, et al., 2012; Poulos, 2010).

A simple KDE is given by:

$$f_h(x) = \frac{1}{nh}\sum_{i=1}^{N} K\left(\frac{x - x_i}{h}\right) \quad (1)$$

where:
N= The number of observations.
h= The bandwidth.
K(x)= The kernel function.
x and x_i= Observations.

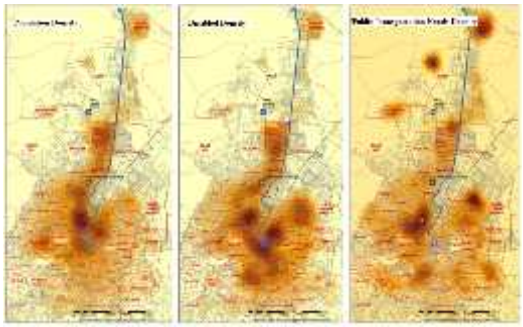

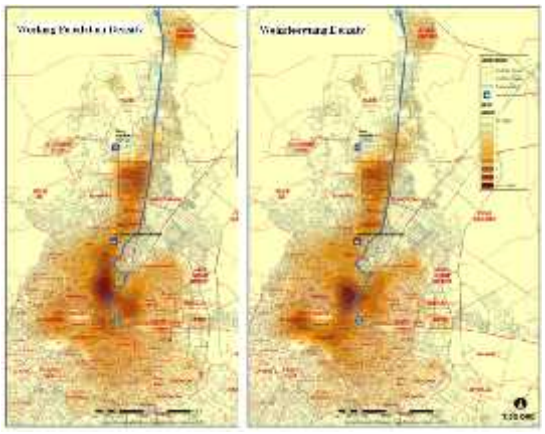

Figure 2. Density maps (left to right: population, disabled, public transportation needs, working population and vehicleowning)

2.2.2. Minibus transportation and GIS-aided production availability parameter across the urban

In this study, types of public transport with minibus transport to analyze the proficiency level on the basis of urban residents and are intended to offer an alternative route. To determine the adequacy of the level of minibus lines, geographically number of people living in buildings and the minibus lines was determined and the necessary database information is processed using GIS software, ArcGIS Desktop 10.0 (Fig. 3). There are 530 minibuses within 28 minibus lines serving Konya's public transportation needs. The total length of these lines is 751 km. Minibuses serve two transfer center throughout the city.

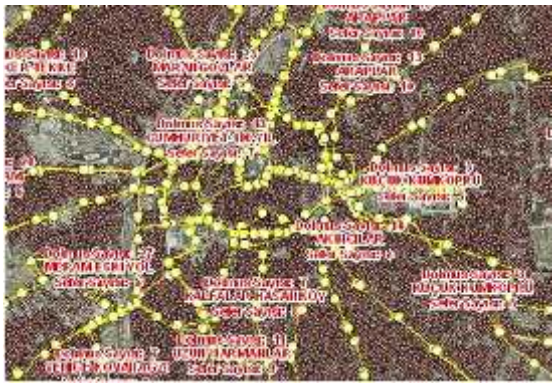

Figure 3. Available minibus lines.

In the study, minibus services to take advantage of every building in the study to determine the value of accessibility to lines 300 m distance; has been identified as the most suitable service distance. 300 m buffer zones were built by ArcGIS software. The domain within 300 m of the buildings were classified according to the degree to which the service. Outside the domain portion were determined the population without adequate benefit levels of minibus transportation services (Fig. 4).

Daily, how many people can be transported by minibus is calculated following formula for production of GIS-based availability parameters of minibus lines.

$$A = p \times q \times 14 \quad (2)$$

Where, A: daily number of transportation people; p: the total number of minibus that uses a line; q: the total number of trips per day and 14: passenger capacity for one minibus.

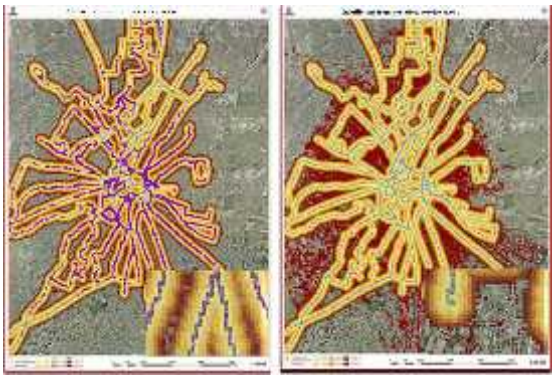

Figure 4. Classification of buildings according to minibus line domain.

Way information which is closest to building and has minibus line is processed in building database. A coefficient for each building is determined with number of people living in the building was proportional to the number of passengers that can be transported. The coefficients obtained for the building was joined with population density (Fig. 5). White area in transportation coefficient density map is transfer center region and minibuses running on all lines pass from this region certainly. When population density map and transport coefficients density map is combined, despite the high population, transport coefficients are seen to be low in the northern region of the city. Again, the difference between population and the transport coefficient values is observed to be higher in the some areas where city's south and west regions.Density analysis was realized for related building in the area that high population density and low transport coefficient. So, priority service areas has emerged (Fig. 6).

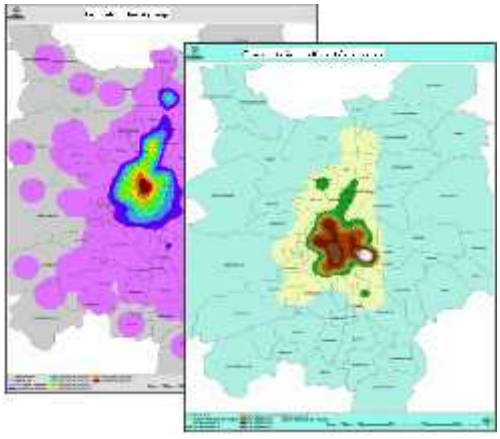

Figure 5. Population and transportation coefficient density maps.

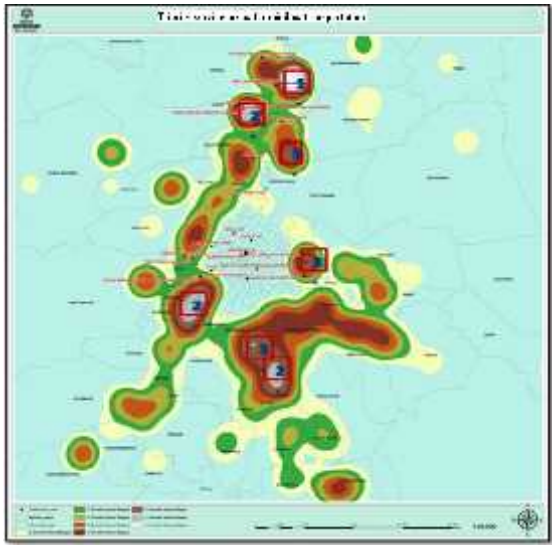

Figure 6. Determined priority service areas for minibus transportation.

2.2.3. Assessment of the current situation of transportation lines and alternative line production with spatial/network analysis methods of northern part of the city

There are 57.3 km total transportation lines using tram and bus of northern part of the city (Fig. 7). Most passengers are transported by tram through these lines. In terms of urban planning, northern part of the city is quite moving. In this region, there is high-density construction.

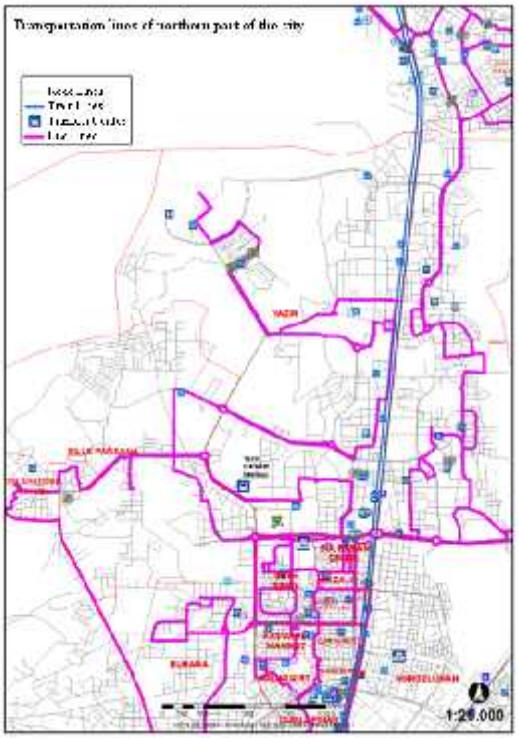

Figure 7. Current situation of transportation lines of northern part of the city.

Obtained analyzes through building using kernel density analysis methods were classified again and the possibility of cross-analysis was obtained. Dominant distribution of data and density distribution according to the load with kernel method were evaluated. The distribution of socio-economic and demographic structure is shown in Figure 8.

Analysis of routing solutions was used Vehicle Routing Problem (VRP) analysis. VRP models and algorithms are vast with many commercial applications. ArcGIS allows users to define a network dataset and a vehicle routing problem (Bozkaya, et al., 2010).

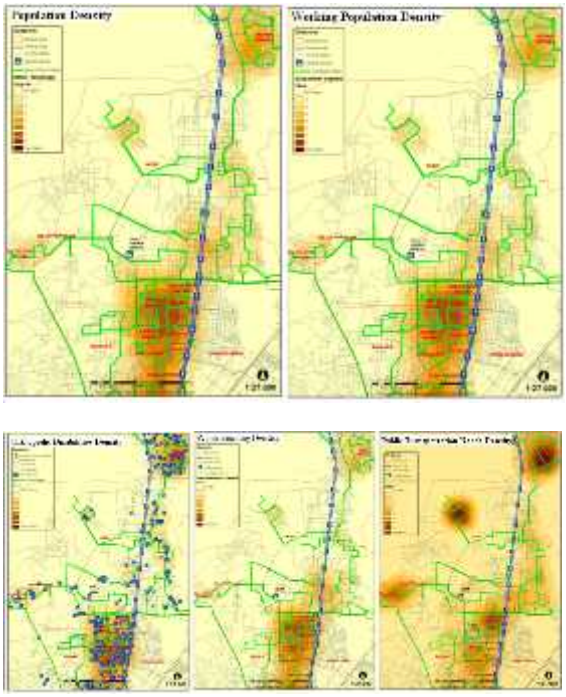

Figure 8. Demographic and socio-economic spatial analysis (Left to right: Population, working population, orthopedic disabilities, vehicleowning and public transportation needs densities)

The VRP is one of the most studied combinatorial optimization problems. VRP is concerned with the optimal design of routes to be used by a fleer of vehicles to serve a set of customers (Golden, et al., 2008). For use in VRP network analysis, generated synthesized map by combining the spatial analysis map in Fig. 8 is shown in Fig. 9. Seen as brown regions indicate areas of appropriate to criteria intersection. The first spatial data is synthesis map for VRP analysis. Active tram line as a second data for VRP analysis was analyzed. Effective service distance of the tram line has been recognized within 3 km considering the existing settlement areas. Also, active usability distance was designated as 300 meters (Fig. 10). 300 m radius was used as the limiting elements for VRP analysis.

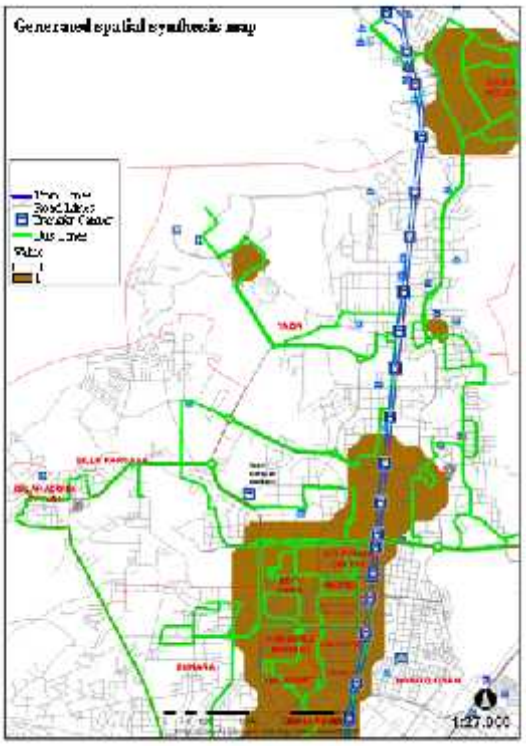

Figure 9. Generated spatial synthesis map for VRP analysis.

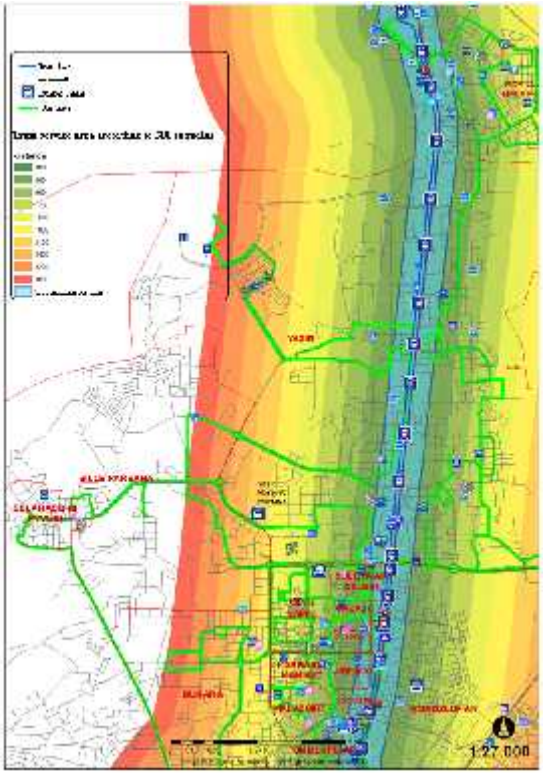

Figure 10. Buffer of tram lines (300 m and 3000 m).

In the northern part of city, the active population areas was determined the third data for VRP analysis. For this process, some regions (such as shopping mall, bus stations, hospital, schools, university, etc.). Evidence needs to be weighted depending on its relative significance. Hence, each location will be evaluated according to weighted criteria, resulting in a ranking on a suitability scale. This method is known as index overlay. In this method, each factor maps will be assigned ranking. Weights are generally assigned to these maps to express the relative importance (Nas, et al., 2010). In this study, highest score have been considered as the most visited for ranking of urban areas. Accordingly, ranking is as follows;

•Shopping mall, city hall, electricity authority, bus stations, hospitals, secondary schools, social welfare institutions, water authority, telecom, university, dormitories=30

•Primary schools, post offices, public enterprises=20

•Military Institute of Health, police stations, , cultural centers, libraries= 10

Formed by the ranking density map is shown in Fig. 11. This map with the synthesis map in Fig. 9 was observed overlapping locally.
Generated maps using spatial analysis are base data for VRP analysis. Within the scope of this data, transportation lines were evaluated again. We have selected the ArcGIS 10.0 software Network Analyst tool for VRP analysis. In this study, VRP analysis was created geometrically the shortest road networks and transportation routes automatically. Before VRP analysis, the total bus route length was 153.2 km in northern part of the city. This length has decreased to 86.7 km after VRP analysis (Fig. 12).

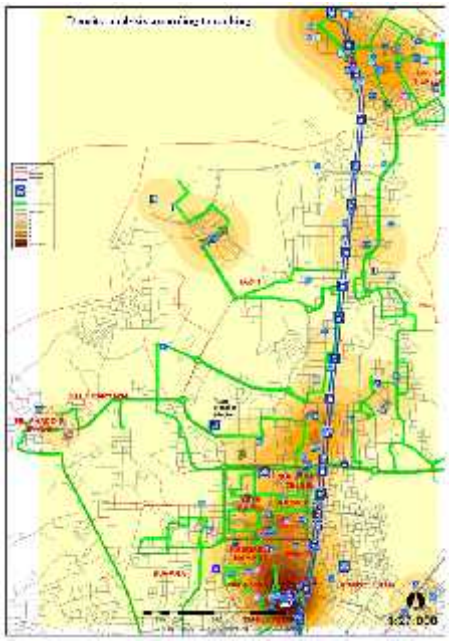

Figure 11. Density analysis according to ranking.

After VRP analysis, structure based transfer center that returning in their own and transferred to the tram line has been proposed for transportation that going to the tram line and the city center, previously. A tram runs every 2 minutes for each tram stations. Transition periods for trams based on the change of the crowd factor based on travel time will be more flexible. Previous case, the cost of only one bus to the municipality for one service is 505.56 Turkish Liras (approximately 243 $). These cost is 286.11 Turkish Liras with spatial and network analysis methods (approximately 138 $). Analysis of the spatial sense regulations realization and detailed bus information (cruises start-to-finish time, passenger capacity, vehicle type, stop, not hours, real speed, etc.) by entering passage costs significantly be reduced with repetitive calibration analysis. Realized spatial arrangements and detailed bus information (start-to-finish time for travel, passenger capacity, vehicle type, speed, etc.) must be entered for this process. In this case, both public transportation can be more efficient and public transportation users will be able to travel more cheaply.

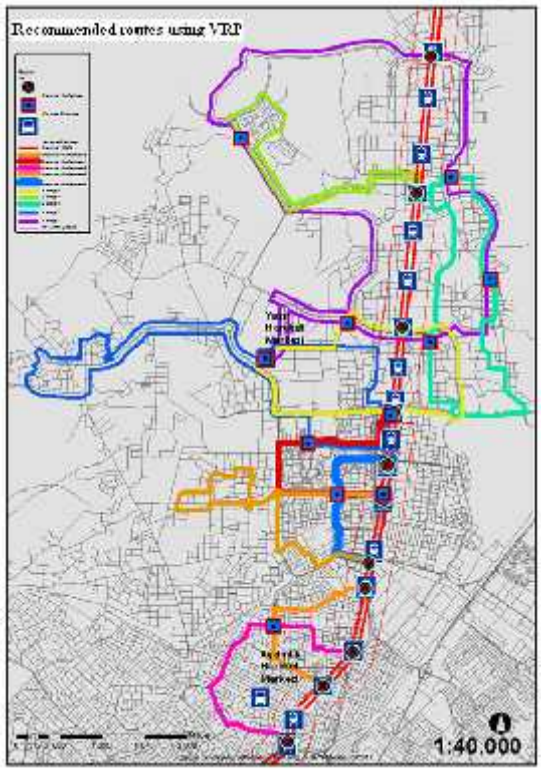

Figure 12. Recommended transportation lines after VRP analysis.

3. RESULTS and DISCUSSION

When adequacy studies was realized for across the city in terms of minibus transportation, most appropriate distance in terms of accessibility to public transportation vehicles for available lines was determined as 300 m walking distance and study was shaped and alternative lines were produced according to the number of persons living in the building for this distance.

Two alternative approaches is developed determining insufficient regions for minibus transportation. The first approach, existing lines is revised within 300 m distance for hight density of population and low public transportation services. Another approach, outside walking distance areas without minibus lines is determined and is the creation of a new minibus lines. According to the first approach, the location of the last stopping point was modified and new lines were added to existing lines. According to the second approach, in areas where population density is high and identified wide roads without minibus lines, new lines have been created.

4. CONCLUSIONS

In this study, the effective use of spatial analysis to rehabilitate bus and minibus transportation appears to constitute an important data. Demand for public transportation is the most important input. However, planning of public transportation with only demand or decision-makers' estimates will reveal many problems over time. Performed public transport policies without knowing spatial distribution of demographic and socio-economic structure of society will begin to deteriorate over time. In this study, performed analysis and synthesis brought about applicability alternatives for public transportation. The aim of this study could be used public transport services for all the people living within the city. To ensure this condition is necessary along with a lot of data to understand the characteristics of the population.

REFERENCES

Bigotte, J.F., Krass, D., Antunes, A.P., Berman, O., 2010. Integrated modeling of urban hierarchy and transportation network planning. Transportation Research Part A 44, 506–522.

Bozkaya, B., Yanik, S., Balcisoy, S., 2010. A GIS-Based Optimization Framework for Competitive Multi-Facility Location-Routing Problem. Netw Spat Econ 10, 297–320

Caulfield, B., Bailey, D., Mullarkey, S., 2013. Using data envelopment analysis as a public transport project appraisal tool. Transport Policy 29, 74–85.

DiJoseph, P., Chien, S.I., 2013. Optimizing sustainable feeder bus operation considering realistic networks and heterogeneous demand. Journal of Advanced Transportation 47, 483–497.

Dorantes, L.M., Paez, A., Vassallo, J.M., 2012. Transportation infrastructure impacts on firm location: the effect of a new metro line in the suburbs of Madrid. Journal of Transport Geography 22, 236–250.

Geng, Y., Ma, M., Xue, B., Ren, W., Liu, Z., Fujita, T., 2013. Co-benefit evaluation for urban public transportation sectorea case of Shenyang, China. Journal of Cleaner Production 58, 82-91.

Golden, B.L., Raghavan, S., Wasil, E.A., 2008. The Vehicle Routing Problem: Latest Advances and New Challenges. Springer, 599.

Gulhan, G., Ceylan, H., Ozuysal, M., Ceylan, H., 2013. Impact of utility-based accessibility measures on urban public transportation planning: A case study of Denizli, Turkey. Cities 32, 102–112.

Gutiérrez-Jarpa, G., Obreque, C., Laporte, G., Marianov, V., 2013. Rapid transit network design for optimal cost and origin–destination demand capture. Computers & Operations Research 40, 3000–3009.

Harris, K., Gende, S.M., Logsdon, M.G., Klinger, T., 2012. Spatial Pattern Analysis of Cruise Ship–Humpback Whale Interactions in and Near Glacier Bay National Park, Alaska. Environmental Management 49, 44–54.

Kim, M., Schonfeld, P., 2013. Integrating bus services with mixed fleets. Transportation Research Part B 55, 227–244.

Kuo, P.F., Lord, D., Walden, T.D., 2013. Using geographical information systems to organize police patrol routes effectively by grouping hotspots of crash and crime data. Journal of Transport Geography 30, 138–148.

Martens, K., Golub, A., Robinson, G., 2012. A justice-theoretic approach to the distribution of transportation benefits: Implications for transportation planning practice in the United States. Transportation Research Part A 46, 684–695.

Mishra, S., Welch, T.F., Jha, M.K., 2012. Performance indicators for public transit connectivity in multi-modal transportation networks. Transportation Research Part A 46, 1066–1085.

Murphy, E., 2012. Urban spatial location advantage: The dual of the transportation problem and its implications for land-use and transport planning. Transportation Research Part A 46, 91–101.

Nas, B., Cay, T., Iscan, F., Berktay, A., 2010. Selection of MSW landfill site for Konya, Turkey using GIS and multi-criteria evaluation. Environmental Monitoring and Assessment 160, 491-500.

Neutens, T., Delafontaine, M., Scott, D.M., Maeyer, P.D., 2012. A GIS-based method to identify spatiotemporal gaps in public service delivery. Applied Geography 32, 253-264.

Sayyady, F., Eksioglu, S.D., 2010. Optimizing the use of public transit system during no-notice evacuation of urban areas. Computers & Industrial Engineering 59, 488–495.

Soh, H., Lim, S., Zhang, T., Fu, X., Lee, G.K.K., Hung, T.G.G., Di, P., Prakasam, S., Wong, L., 2010. Weighted complex network analysis of travel routes on the Singapore public transportation system. Physica A 389, 5852–5863.

Timilsina, G.R., Dulal, H.B., 2011. Urban Road Transportation Externalities: Costs and Choice of Policy Instruments. The World Bank Research Observer 26, 162-191.

Uyan, M, 2013. MSW landfill site selection by combining AHP with GIS for Konya, Turkey. MSW landfill site selection by combining. Environmental Earth Sciences, DOI 10.1007/s12665-013-2567-9.

Yang, J., Ferreira, J., 2009. Informing the public of transportation–land use connections. Transportation Research Part C 17, 27–37.

Zhou, J., Chen, C.L.P., Chen, L., Zhao, W., 2013. A User-Customizable Urban Traffic Information Collection Method Based on Wireless Sensor Networks. IEEE Transactions on Intelligent Transportation Systems 14, 1119-1128.

International Journal of Engineering and Geosciences (IJEG),
Vol;2, Issue;01, pp. 35-40, February, 2017, ISSN 2548-0960, Turkey,
DOI: 10.26833/ijeg.287308

THE EFFECT OF JPEG COMPRESSION IN CLOSE RANGE PHOTOGRAMMETRY

Akcay, O.[1*], Erenoglu, R. C.[1], Avsar, E. O.[1]

[1] Canakkale Onsekiz Mart University, Engineering Faculty,
Department of Geomatics Engineering, Tel: +90 286 2180018/2201, 17100, Canakkale, Turkey
(akcay@comu.edu.tr, ceren@comu.edu.tr, ozguravsar@comu.edu.tr)

*Corresponding Author, Received: 13/01/2017, Accepted: 28/01/2017

ABSTRACT: Digital photogrammetry, using digital camera images, is an important low-cost engineering method to produce precise three-dimensional model of either an object or the part of the earth depending on the image quality. Photogrammetry which is cheaper and more practical than the new technologies such as LIDAR, has increased point cloud generation capacity during the past decade with contributions of computer vision. Images of new camera technologies needs huge storage space due to larger image file sizes. Moreover, this enormousness increases image process time during extraction, orientation and dense matching. The Joint Photographic Experts Group (JPEG) is one of the most commonly used methods as lossy compression standard for the storage purposes of the oversized image file. Particularly, image compression at different rates causes image deteriorations during the processing period. Therefore, the compression rates affect accuracy of photogrammetric measurements. In this study, the close range images compressed at the different levels were investigated to define the compression effect on photogrammetric results, such as orientation parameters and 3D point cloud. The outcomes of this study show that lower compression ratios are acceptable in photogrammetric process when moderate accuracy is sufficient.

Keywords: *Photogrammetry, JPEG, compression, 3D modeling, image matching, exterior orientation*

1. INTRODUCTION

Photogrammetry includes scientific methodologies that calculate the three-dimensional coordinates of an object via measuring corresponding points on the overlapping images. The mathematical relation between an image point and an object point is derived by collinearity equations that based on central projection (Kyle, 2013). The recent integration of computer vision algorithms and photogrammetric methods is leading to interesting procedures which have increasingly automated the entire image-based 3D modelling process (Remondino et al., 2014). In last two decades, Close-Range Photogrammetry (CRP) as a contribution of photogrammetry and computer vision, spread into many fields of engineering applications such as medical modelling applications (Xiao et al., 2014), orthophotos by Unmanned Aerial Systems (UAS) (Akcay, 2015) and documentation of cultural heritages (Yılmaz et al., 2007). Three dimensional textured models, digital surface models and true orthophotos can be produced using advantages of low-cost CRP software.

CRP software implement automatic point detection and robust matching algorithms for photogrammetric process. The most common algorithm; Scale Invariant Feature Transform (SIFT) is a digital property extraction method that allows automatic identification of characteristic points (Lowe, 2004). Bay et al. (2006), developed Speeded Up Robust Features (SURF), that approximate SIFT algorithm with respect to repeatability, distinctiveness, and robustness, yet can be computed and compared much faster. This is achieved by relying on integral images for image convolutions; by building on the strengths of the leading existing detectors and descriptors by using a Hessian matrix-based measure for the detector, and a distribution-based descriptor. But these algorithms might be inadequate when very high accuracy (sub-pixel) is necessary, such as industrial (Luhmann et al., 2015) and engineering photogrammetric measurements (Avsar et al, 2015). Traditional photogrammetric measurement is to mark corresponding points manually, which requires more time-consuming and labour-intensive process. Furthermore, the accuracy of the manual measurement depends on user experience and therefore required product quality may not be achieved. Third measurement method in CPR is the automatic measurement of specially coded targets within sub-pixel accuracy. These approximations depend on combined usage of normalised cross correlation and least square image matching. The size and shape of the specially coded targets are determined according to camera-object distance (Yılmaztürk, 2011).

After image orientation implementation, all three mentioned methods produce three-dimensional model from point cloud by Multi-view stereo (MVS) (Seitz et al., 2006). Multi-view stereo algorithms provide feature detection and are able to construct highly detailed 3D models from multiple images (Furukawa and Ponce, 2007).

Raw data format is the uncompressed or possibly least processed format of the images obtained by digital cameras or scanners. Besides raw formats; camera manufacturers provide lower-file size and high-quality Joint Photographic Experts Group (JPEG) (Hamilton, 1992) and its derivative such as JPEG2000 (Christopouloset al., 2000) images by embedded image processing software in digital camera (Hamilton, 1992). Today, new generation photogrammetric software can process both raw and compressed image files.

Many processing steps applied sequentially while getting JPEG images. First, the colour space conversion is performed. Red, Green, Blue (RGB) image within the visible wavelength color-coded format is converted to $Y'C_bC_r$ (Y' is luma component and C_b, C_r are two chroma components) expressed in the colour space. Colour space conversion, is defined in ITU-R BT.601 standard, previously called CC 601. In second step of the JPEG conversion, especially the colour sub-sampling process is performed to reduce the data flow rate (Kerr, 2012). In the third step, each channel of the image with the block parsing process is divided into 8x8 or 16x16 blocks. The two-dimensional discrete cosine transform (DCT) is applied on each block to determine the energy distribution (Ahmed et al., 1974). Finally, entropy coding with Huffman is calculated for each block (Huffman, 1952) after quantization step is implemented.

Cronk (2001) in his study examined the effect of JPEG compression in CRP. Yılmaztürk and Akcay (2005) examined the JPEG compression effect on the sub-pixel measurement by using different target sizes. Beside photogrammetric studies, Liang et al. (2006) discussed the effect of compression on remote sensing processes. In the study, the effect of different JPEG image compression ratios on the accuracy of the photogrammetric evaluation and generation of three-dimensional point cloud were examined.

2. METHODOLGY AND APPLICATION

2.1 Exterior orientation with different methods

In order to compare the different photogrammetric measurement methods (manual, SURF and coded targets) explained in the introduction; a statue in the university campus was selected as the study object. The raw images were acquired with a 18MP Canon EOS 650D without compression. 37 acquired images were evaluated during the study. The images were oriented according to the mentioned methods (Table 1).

Table 1. Comparison of exterior orientation parameters

Method	**Mean square error (m)**			**# points (avg)**
	X	Y	Z	
Manual	0.00090	0.00063	0.00084	29
SURF	0.01041	0.00654	0.00957	680
Coded T.	0.00096	0.00066	0.00087	18

Method	**Mean square error (degree)**		
	Omega	Phi	Kappa
Manual	0.03295	0.02586	0.03678
SURF	0.05423	0.04119	0.06233
Coded T.	0.03409	0.02654	0.03958

SURF algorithm is able to define characteristic features which have intensive radiometric and spatial changes (Figure 1). As shown in Table 1; approximately 680 points matched in images with SURF algorithm which is 25-35 times more than two other measurement methods. On the contrary; SURF algorithm delivers mean square error of exterior orientation parameters ten times greater than others.

Similar accuracy results were obtained in orientation when coded targets and manual measurement were compared.

Figure 1. SURF feature extraction results.

2.2. Application of Image Compression

The effect of the compression was considered for automatic measurement methods. Therefore, manual measurements were not examined for the compressed images. On the other hand, SURF and coded targets as automatic measurement methods were accounted for different compression levels. Raw data format was converted to JPEG compressed files to obtain ten percentage gradual decreased quality images.

Compression rates especially decreases the amount of the extracted features as well as robust matching number (Chao et al., 2013). However, results showed an unworthy decline in the context of extracted features due to quality loss as shown in Figure 2.

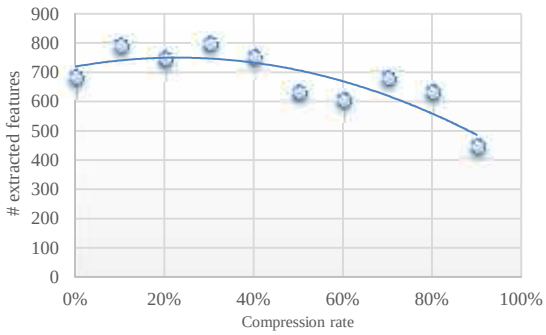

Figure 2. SURF feature extraction results.

Consideration of the extracted features at different compression levels might not be enough in order to infer the influence of the compression. Understanding of the matching performance is also important beside the feature extraction. Low matching performance is clearly seen at more than forty percentage compression rates when Figure 3 is inspected.

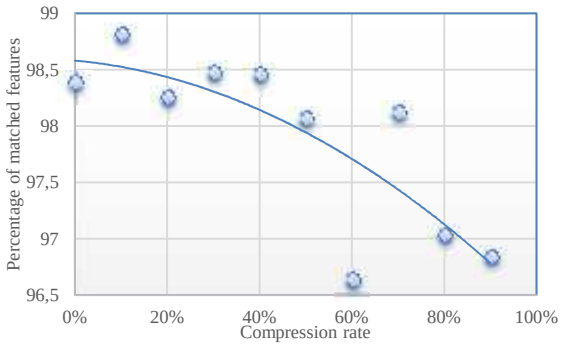

Figure 3. Matched points for SURF.

Coded targets which provide sub-pixel accuracy matching do not give the possibility of an appropriate compression analysis. Automatic photogrammetric measurement with coded target is vulnerable to compression process as the mentioned method is so sensitive to image quality. More than twenty percentage compression makes the photogrammetric calculation failure because of the insufficient matched coded target.

3. DISCUSSION

3.1. Exterior orientation with different methods

In the study, mean square errors (MSE) of the exterior orientation obtained using automatic measurement methods were also compared at each compression levels. Figure 4 illustrates MSE of the projection centre coordinates X_0,Y_0,Z_0 calculated using SURF extraction and matching while Figure 5 indicates MSE of the orientation angles ϖ,φ,κ. As seen in Figure 4, errors of projection centre coordinates sharply increase after forty percent compression level. Figure 5 also indicates that forty percentage compression is determining level during the computation of the rotation angles.

Figure 4. SURF feature extraction results.

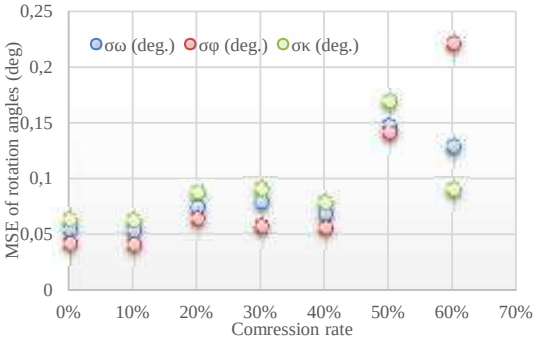

Figure 5. SURF feature extraction results.

An appropriate compression analysis of exterior orientation with coded targets is as not possible as computed with SURF algorithm. Orientations computed with sub-pixel measurement accuracy showed significant deficiencies at low compression rates. Moreover, high compression rates more than twenty percent were not possible to define orientation values. Figures 6 and 7 illustrate that the quality change in images had little effect on orientation accuracy.

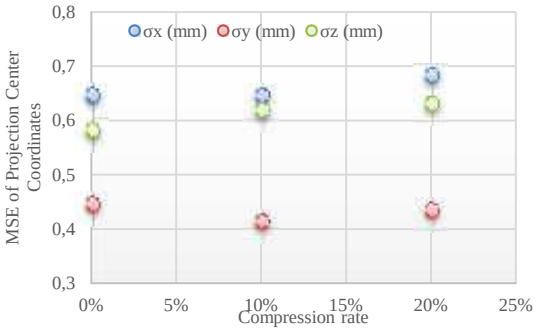

Figure 6. Coded targets feature extraction results.

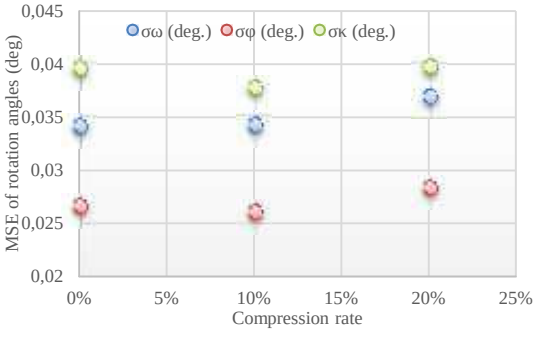

Figure 7. Coded targets feature extraction results.

3.2. Point cloud generation

Point cloud generation is implemented with MVS also known as dense matching using multiple images. Accuracy of the obtained point is related with the number and angle of image. Figure 8 shows a part of the point cloud from the statue. As it is seen in the figure, point cloud is so dense. Consequently, the photogrammetric point cloud might be a low-cost alternative to LIDAR point cloud in some cases (Nouwakpo et al., 2015).

Figure 8. Point Cloud produced by MVS from SURF results.

Applied compression levels also affect results of MVS point cloud beside exterior orientation. This affect emanates from both faulty exterior orientation results and MVS processing with low resolution images. At the high compression levels, gross errors were observed on the point clouds. Figure 9 shows a point cloud which was obtained in fifty percent compression level. The figure explicitly illustrates the failures on the point cloud. However low compression levels less than fifty percent output more stable point clouds as indicated in Figure 10.

Figure 9. Gross errors of point cloud obtained from %50 compressed images by SURF.

Figure 10. 3D model obtained from %20 compressed images by SURF.

As MVS results were investigated for each compression level, point numbers generated in the clouds were decreased due to higher compression levels. Particularly, numbers of points diminished at the compression higher than thirty percent. On the contrary, the triangulation and filtered point clouds remained still despite compression (Figure 11). Because triangulation and filtered point cloud were computed independently from images, they were not influenced as much as the original point clouds. Gross errors on the MVS point cloud, also reflect the distortions to the textured models.

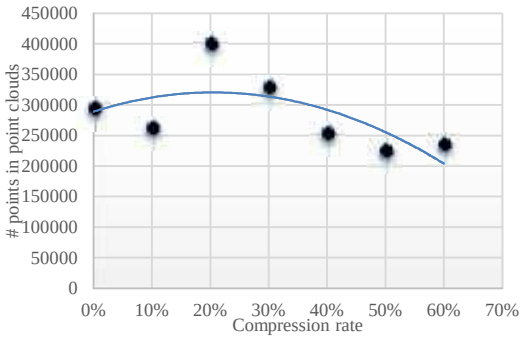

Figure 11. Compression-point graph.

4. RESULTS AND RECOMMENDATIONS

In the experimental tests, it has been shown that the low compression ratios have a negligible effect on the photogrammetric process. On the other hand, if it is considered that a small amount of compression rates can be seriously reduced in file sizes, up to twenty or thirty percent of compression ratio, the photogrammetric modelling been has proved to be problem-free for the works that do not require high precision. However, sub-pixel measurement method showed bad results with low compressed images as the method needed high resolution.

In the case of high compression ratios, the three orientation methods applied also considerably reduced the precision of the exterior orientation and caused significant rough errors in the 3D models. It has been observed that the number of point clouds decreases considerably after thirty percent compression.

No colour subsampling is done in JPEG compression performed in this study. By applying the colour subsample in many different combinations, its effect on the photogrammetry can be revealed in future studies. Also in future work, TIFF format and JPEG compression formats, which are obtained without loss from the raw data format, can be compared. Although JPEG is one of the most used standards, the impact on photogrammetric evaluation of other popular image compression algorithms such as JPEG2000 should be discussed.

ACKNOWLEDGMENTS

This study was supported by Canakkale Onsekiz Mart University, Scientific Research Projects Coordination Unit [grant number FBA-2013-109].

REFERENCES

Ahmed N., Natarajan T., and Rao K., 1974. Discrete cosine transform, IEEE Trans. Comput., vol. C-23, pp.90 -93 1974.

Akcay, O., 2015. Landslide Fissure Inference Assessment by ANFIS and Logistic Regression Using UAS-Based Photogrammetry. ISPRS International Journal of Geo-Information, 4(4), 2131-2158.

Avsar, E. Ö., Altan, M. O., Doğan, Ü. A., and Akça, D., 2015. Determining Pull-Out Deformations by Means of an Online Photogrammetry Monitoring System. International Journal of Environment and Geoinformatics, 2(1).

Bay, H., Tuytelaars, T., and Van Gool, L., 2006. Surf: Speeded up robust features. In Computer vision–ECCV 2006 pp. 404-417. Springer Berlin Heidelberg.

Chao, J., Chen, H., and Steinbach, E., 2013. On the design of a novel JPEG quantization table for improved feature detection performance. In Image Processing (ICIP), 2013 20th IEEE International Conference on (pp. 1675-1679). IEEE.

Christopoulos, C.A. , Skodras, A.N. and Ebrahimi, T., 2000. The JPEG 2000 still image coding system: An overview, IEEE Trans. Consumer Electron, vol. 46, pp.1103 -1127 2000.

Cronk S., 2001. The Effects of JPEG Image Compression On Digital Close-Range Photogrammetry, Report, Melbourne.

Furukawa Y. and Ponce J., 2007 Accurate, Dense, and Robust Multi-View Stereopsis, CVPR 2007.

Hamilton. E., 1992. JPEG File Interchange Format - Version 1.02. C-Cube Microsystems, Sep 1992.

Huffman, D. A., 1952. A method for the construction of minimum redundancy codes, Proc. IRE, vol. 40, pp.1098 -1101 1952.

Kerr D. A., 2012. Chrominance Subsampling in Digital Images.
http://dougkerr.net/pumpkin/articles/Subsampling.pdf, Jan. 2012.

Kyle, S., 2013. Close-Range Photogrammetry and 3D Imaging; Walter de Gruyter: Berlin, Germany; ISBN-ISSN: 9783110302783.

Liang Z. , Xinming T. and Lin L., 2006. Effects of JPEG 2000 compression on remote sensing image quality, In Proc. of IEEE International Geoscience and Remote Sensing Symposium, pp. 3297-3300, July 2006.

Luhmann, T., Fraser, C., and Maas, H. G., 2015. Sensor modelling and camera calibration for close-range photogrammetry. ISPRS Journal of Photogrammetry and Remote Sensing.

Lowe, D. G., 2004. Distinctive image features from scale-invariant keypoints., International Journal of Computer Vision, 60, 2, pp. 91-110.

Nouwakpo, S. K., Weltz, M. A., and McGwire, K., 2015. Assessing the performance of structure- from-motion photogrammetry and terrestrial LiDAR for reconstructing soil surface microtopography of naturally vegetated plots. Earth Surface Processes and Landforms. 41(3) 308-322.

Remondino, F., Spera, M.G., Nocerino, E., Menna, F. and Nex, F., 2014. State of the art in high density image matching. Photogramm. Rec., 29, 144–166.

Seitz, S. M., Curless, B., Diebel, J., Scharstein, D., and Szeliski, R., 2006. A comparison and evaluation of multi-view stereo reconstruction algorithms. In Computer vision and pattern recognition, 2006 IEEE Computer Society Conference on, 1, 519-528. IEEE.

Xiao, K., Zardawi, F., van Noort, R., and Yates, J. M., 2014. Developing a 3D colour image reproduction system for additive manufacturing of facial prostheses. The International Journal of Advanced Manufacturing Technology, 70(9-12), 2043-2049.

Yilmaz, H. M., Yakar, M., Gulec, S. A., and Dulgerler, O. N., 2007. Importance of digital close-range photogrammetry in documentation of cultural heritage. Journal of Cultural Heritage, 8(4), 428-433.

Yılmaztürk, F., 2011. Full-automatic self-calibration of color digital cameras using color targets. Optics express, 19(19), 18164-18174.

Yılmaztürk F., Akçay Ö., 2005. Jpeg Görüntü Sıkıştırmanın Yakın Mesafe Dijital Fotogrametri Üzerindeki Etkileri, s. 918-925, 10. Türkiye Harita Bilimsel ve Teknik Kurultayı, Ankara, Türkiye, 28.03.2005 - 01.04.2005.